

Measurement of charged particle spectra in minimum-bias events from proton–proton collisions at $\sqrt{s} = 13$ TeV

CMS Collaboration*

CERN, 1211 Geneva 23, Switzerland

Received: 28 June 2018 / Accepted: 8 August 2018 / Published online: 31 August 2018
© CERN for the benefit of the CMS collaboration 2018

Abstract Pseudorapidity, transverse momentum, and multiplicity distributions are measured in the pseudorapidity range $|\eta| < 2.4$ for charged particles with transverse momenta satisfying $p_T > 0.5$ GeV in proton–proton collisions at a center-of-mass energy of $\sqrt{s} = 13$ TeV. Measurements are presented in three different event categories. The most inclusive of the categories corresponds to an inelastic pp data set, while the other two categories are exclusive subsets of the inelastic sample that are either enhanced or depleted in single diffractive dissociation events. The measurements are compared to predictions from Monte Carlo event generators used to describe high-energy hadronic interactions in collider and cosmic-ray physics.

1 Introduction

The study of the properties of particle production without any selection bias arising from requiring the presence of a hard scattering (a selection known as “minimum bias”) is one of the most basic measurements that can be made at hadron colliders. Such events are produced by strong interactions of partons inside the hadrons, which occur at low momentum exchanges, for which predictions of quantum chromodynamics (QCD) cannot be obtained perturbatively, and for which diffractive scatterings or multiple partonic interactions (MPI) play a significant role. The theoretical description of these components of particle production is based on phenomenological models with free parameters adjusted (“tuned”) to reproduce the experimental data. However, when a momentum transfer of several GeV (referred to as a hard process) is involved, predictions obtained from perturbative QCD (pQCD) are, in many cases, in good agreement with the measurements. Understanding the transition region between hard processes calculable with perturbative techniques and soft processes described by nonperturbative models is required for a full description of particle production in proton–proton (pp) collisions at the LHC. It is also essential when the col-

lider is operated at high luminosities since a bunch crossing contains many pp collisions (pileup) forming a complex final state that needs to be theoretically controlled for precise studies of standard model processes, as well as for new physics searches.

Inclusive measurements of charged particle pseudorapidity distributions, $dN_{\text{ch}}/d\eta$, and transverse momentum distributions, dN_{ch}/dp_T , as well as charged particle multiplicities have been previously performed in proton–proton and proton–antiproton collisions in the center-of-mass energy range $\sqrt{s} = 0.2$ –8 TeV and in various phase space regions [1–19]. Most of these measurements are described to within 10–20% by present event generators as reported, e.g., in Ref. [20].

More recently, measurements of the charged-hadron pseudorapidity distribution in pp collisions at the highest energies reached so far, $\sqrt{s} = 13$ TeV, have been presented in Refs. [21–24]. The present work extends those studies, for charged particles with $p_T > 0.5$ GeV measured over the range $|\eta| < 2.4$, to cover not only the pseudorapidity density, but also the per-event multiplicity probability, $P(N_{\text{ch}})$, as well as different transverse-momentum distributions, such as that of the leading charged particle dN_{ch}/dp_T , and its corresponding integrated spectrum, $D(p_{T,\text{min}})$. The integrated spectrum $D(p_{T,\text{min}})$ is defined as:

$$D(p_{T,\text{min}}) = \frac{1}{N_{\text{events}}} \int_{p_{T,\text{min}}} dp_{T,\text{leading}} \left(\frac{dN}{dp_{T,\text{leading}}} \right). \quad (1)$$

Here N_{events} is the number of selected events, N is the number of events with a leading charged particle with transverse momentum $p_{T,\text{leading}}$, and $p_{T,\text{min}}$ is the lower limit of the integral. In each event, the highest- p_T charged particle within $|\eta| < 2.4$ and with $p_T > 0.5$ GeV is selected as the leading charged particle. The integrated spectrum of charged particles is sensitive to the transition between the nonperturbative and perturbative QCD regions [17, 25].

The measured distributions are presented for three different event data sets: an inelastic sample, a sample dominated

* e-mail: cms-publication-committee-chair@cern.ch

by nonsingle diffractive dissociation events (NSD-enhanced sample), and a sample enriched by single diffractive dissociation events (SD-enhanced sample). The measurements are compared to predictions from different Monte Carlo (MC) event generators used to describe high-energy hadronic interactions in collider and cosmic-ray physics.

This article is organized as follows. Section 2 gives a brief description of the CMS detector. The MC models used for corrections and comparison to data are described in Sect. 3. The data sample, track reconstruction, and event selection are discussed in Sect. 4. The procedure to correct the data for detector effects and the systematic uncertainties affecting the measurements are described in Sects. 5 and 6, respectively. The final results are presented in Sect. 7 and a summary is given in Sect. 8.

2 The CMS detector

The central feature of the CMS apparatus is a superconducting solenoid of 6 m internal diameter, providing a magnetic field of 3.8 T. Within the solenoid volume are a silicon pixel and strip tracker, a lead tungstate crystal electromagnetic calorimeter, and a brass and scintillator hadron calorimeter, each composed of a barrel and two endcap sections. Forward calorimeters extend the pseudorapidity coverage provided by the barrel and endcap detectors. Muons are detected in gaseous ionization chambers embedded in the steel flux-return yoke outside the solenoid.

The tracking detector consists of 1440 silicon pixel and 15 148 silicon strip detector modules. The barrel is composed of 3 pixel and 10 strip layers around the primary interaction point (IP) at radii ranging from 4.4 to 110 cm. The forward and backward endcaps each consist of 2 pixel disks and 12 strip disks in up to 9 rings. Three of the strip rings and four of the barrel strip layers contain an additional plane, with a stereo angle of 100 mrad, to provide a measurement of the r - and z -coordinate, respectively. The silicon tracker measures charged particles within the pseudorapidity range $|\eta| < 2.5$. For particles of $1 < p_T < 10$ GeV and $|\eta| < 1.4$, the track resolutions are typically 1.5% in p_T and 25–90 (45–150) μm in the transverse (longitudinal) impact parameter [26].

The hadron forward (HF) calorimeter uses steel as an absorber and quartz fibers as the sensitive material. The HF calorimeters are located at 11.2 m from the interaction region, one on each end, and together they provide coverage in the range $2.9 < |\eta| < 5.2$. Each HF calorimeter consists of 432 readout towers, containing long and short quartz fibers running parallel to the beam. The long fibers run the entire depth of the HF calorimeter (165 cm, or approximately 10 interaction lengths), while the short fibers start at a depth of 22 cm from the front of the detector. By reading out the two sets of fibers separately, it is possible to distinguish showers gener-

ated by electrons and photons, which deposit a large fraction of their energy in the long-fiber calorimeter segment, from those generated by hadrons, which produce on average nearly equal signals in both calorimeter segments. Calorimeter towers are formed by grouping bundles of fibers of the same type. Bundles of long fibers form the electromagnetic towers and bundles of short fibers form the hadronic towers.

A more detailed description of the CMS detector, together with a definition of the coordinate system used and the relevant kinematic variables, can be found in Ref. [27].

3 The theoretical predictions

Three different event generators simulating hadronic collisions are used to correct the measurements to particle level (Sect. 5), and for comparisons with the final results. Simulated event samples were used to optimize the event selection, vertex selection, and tracking efficiencies.

The PYTHIA8 (version 8.153) event generator [28] uses a model [28,29] in which initial-state radiation and multiple partonic interactions are interleaved. Parton showers in PYTHIA are modeled according to the Dokshitzer–Gribov–Lipatov–Altarelli–Parisi (DGLAP) evolution equations [30–32], and hadronization is based on the Lund string fragmentation model [33]. Diffractive cross sections are described by the Schuler–Sjöstrand model [34]. Particle production from a low-mass state X , with $M_X < 10$ GeV, is described by the Lund string fragmentation model, while for higher masses, $M_X > 10$ GeV, a perturbative description of the pomeron–proton scattering is introduced. The latter is based on diffractive parton distribution functions [35–37], which represent probability distributions for partons inside the proton, under the constraint that the proton emerges intact from the collision. The PYTHIA8 generator is used with the tune CUETP8M1 [20] (also referred to as CUETM1), which is based on the Monash tune [38] using the NNPDF2.3LO [39,40] parton distribution function (PDF) set, with parameters optimized to reproduce underlying event (UE) data from CMS at $\sqrt{s} = 7$ TeV and CDF at $\sqrt{s} = 1.96$ TeV.

The minimum bias Rockefeller (MBR) model [41] is also implemented within the PYTHIA8 event generator. When used in conjunction with the 4C tune [42] (which includes parton showering) it is referred to as the PYTHIA8 MBR4C model. This model reproduces the measured energy dependence of the total, elastic, and inelastic pp cross sections, and can be used to fully simulate the main diffractive components of the inelastic cross section. The generation of diffractive processes is based on a phenomenological renormalized Regge model [43,44], interpreting the pomeron flux as the probability of forming a diffractive rapidity gap. The value of the pomeron intercept $\alpha(0) = 1.08$ is found to give the best

description of the diffractive dissociation cross sections measured by CMS at $\sqrt{s} = 7$ TeV [45].

The data are also compared to predictions from the EPOS [46] MC event generator (version 1.99) used in cosmic ray physics [47], including contributions from soft- and hard-parton dynamics. The soft component is described in terms of the exchange of virtual quasi-particle states, as in Gribov's Reggeon field theory [48], with multi-pomeron exchanges accounting for UE effects. At higher energies, the interaction is described in terms of the same degrees of freedom (reggeons and pomerons), but generalized to include hard processes via hard-pomeron scattering diagrams, which are equivalent to a leading order pQCD approach with DGLAP evolution. The EPOS generator is used with the LHC tune [49,50].

Event samples obtained from the event generators PYTHIA8, PYTHIA8 MBR, and EPOS are passed through the CMS detector simulation based on GEANT4 [51], and are processed and reconstructed in the same manner as collision data. The number of pileup interactions in the MC samples is adjusted to match the distribution in the data.

4 Data set, track reconstruction, and event selection

In order to minimize the effect of pileup, the data considered in the analysis were collected in a special run in summer 2015 with an average number of pp interactions per bunch crossing of 1.3 [52].

The two LHC beam position monitors closest to the IP for each LHC experiment, called the beam pick-up timing experiment (BPTX) detectors, are used to trigger the detector readout. They are located around the beam pipe at a distance of 175 m from the IP on either side, and are designed to provide precise information on the bunch structure and timing of the incoming beams. Events are selected by requiring the presence of both beams crossing at the IP, as inferred from the BPTX detectors.

The CMS track reconstruction algorithm is based on a combinatorial track finder (CTF) [53]. The collection of reconstructed tracks is obtained through multiple iterations of the CTF reconstruction sequence. The iterative tracking sequence consists of six iterations. The first iteration is designed to reconstruct prompt tracks (originating near the pp interaction point) with three pixel hits and $p_T > 0.8$ GeV. The subsequent iterations are intended to recover prompt tracks that only have two pixel hits or lower p_T . At each iteration an extrapolation of the trajectory is performed, and using the Kalman filter, additional strip hits compatible with the trajectory are assigned.

High-purity tracks [26] are selected with a reconstructed $p_T > 0.5$ GeV, in order to have high tracking efficiency (>80%) and a relative transverse momentum uncertainty

smaller than 10%. Tracks are measured within the pseudorapidity range $|\eta| < 2.4$ corresponding to the fiducial acceptance of the tracker, in order to avoid effects from tracks very close to its geometric edge at $|\eta| = 2.5$. The impact parameter with respect to the beam spot in the transverse plane, d_{xy} , is required to satisfy $|d_{xy}/\sigma_{xy}| < 3$, while for the point of closest approach to the primary vertex along the z -direction, (d_z), the requirement $|d_z/\sigma_z| < 3$ is imposed. Here σ_{xy} and σ_z denote the uncertainties in d_{xy} and d_z , respectively. The number of pixel detector hits associated with a track has to be at least 3 in the pseudorapidity region $|\eta| \leq 1$ and at least 2 for $|\eta| > 1$.

Rejection of beam background events and events with more than one collision per bunch crossing is achieved by requiring exactly one reconstructed primary vertex [26]. The vertex produced by each collision is required to be within $|z| < 15$ cm with respect to the center of the luminous region along the beamline and within 0.2 cm in the transverse direction.

Different event classes are defined based on activity in the HF calorimeters by requiring the presence of at least one tower with an energy above the threshold value of 5 GeV in the fiducial acceptance region, $3 < |\eta| < 5$. The veto condition is defined by an energy deposit in the towers less than a given threshold value. An inelastic sample consists of events with activity on at least one side of the calorimeters, whereas an NSD-enhanced sample contains those with calorimeter activity on both sides. An SD-enhanced sample is defined by requiring activity on only one side of the calorimeters, with a veto condition being applied to the other side.

The HF energy threshold of 5 GeV was determined from the measurement of electronic noise and beam-induced background in the HF calorimeters, using an event sample for which a single beam was circulating in the LHC ring, and an event sample without beams. The threshold of 5 GeV keeps the background due to noise low, while still maintaining a high selection efficiency. The fraction of events with at least one HF tower on either side of the detector with an energy above the threshold of 5 GeV in the event samples with no collisions (one beam or no beam) is 0.13%. The efficiency of the event selection defined by the presence of at least one tower with an energy above 5 GeV in either side of the calorimeters is 99.3%, and is calculated with respect to the event sample defined by the presence of exactly one reconstructed primary vertex.

In total a sample of 2.23 million events is selected containing 2 million NSD events and 0.23 million SD-enhanced events.

Table 1 Summary of stable-particle level definitions for each of the event samples, corresponding to the inelastic, the NSD-enhanced, and SD-enhanced categories. Charged particles are selected with $p_T > 0.5$ GeV and $|\eta| < 2.4$. Forward trigger particles correspond to those with energy $E > 5$ GeV located in side^- (defined as $-5 < \eta < -3$) and/or side^+ (defined as $3 < \eta < 5$). Similarly, a veto corresponds to the absence of a trigger particle with $E > 5$ GeV in side^- and/or side^+

Event sample	Forward region energy selection
Inelastic	Trigger particle in side^- or side^+
NSD-enhanced	Trigger particle in side^- and side^+
SD-enhanced	Trigger particle in side^- (side^+) and veto in side^+ (side^-)

5 Correction to particle level

The data are corrected for tracking and event selection efficiencies, as well as for detector resolution effects. The corrected distributions correspond to stable primary charged particles, which are either directly produced in pp collisions or result from decays of particles with decay length < 1 cm. At particle level, events are selected if at least one charged particle is found within $|\eta| < 2.4$ and $p_T > 0.5$ GeV. The different event selections are defined in a similar manner to how they are defined at detector level in order to avoid any bias towards a specific MC model. Activity in the forward region is defined by the presence of at least one particle, either charged or neutral, with an energy above 5 GeV in the region $3 < |\eta| < 5$ (referred to as the trigger particle). The veto condition is equivalently defined by the absence of particles with an energy above 5 GeV. The inelastic data set is defined by requiring a trigger particle in the pseudorapidity range $3 < \eta < 5$ or $-5 < \eta < -3$. The NSD-enhanced event sample is defined by requiring a trigger particle in the regions $3 < \eta < 5$ and $-5 < \eta < -3$. The SD-enhanced event sample is defined by requiring a trigger particle in either the positive or negative η range, with the veto condition applied to the other region. The SD-enhanced event sample is further divided into two exclusive subsets according to the η region in which the trigger particle is detected. These subsets are referred to as SD-One-Side enhanced event samples. Table 1 shows a summary of the event selection definitions at particle level.

A response matrix, R , is constructed using the information provided by the MC event generators and by the full detector simulation. The elements of the response matrix (R_{ji}) represent the conditional probability that (for a given observable) a true value i is measured as a value j . In this analysis, two different correction procedures were implemented. The first method (method 1) makes use of the full detector simulation, while in the second method (method 2) a parametrization of the detector response is implemented in order to over-

come the statistical limitations of the full detector simulation. Whenever it is possible to accurately parametrize the detector resolution, method 2 is used, otherwise method 1 is applied. The two implemented methods account for unreconstructed particles (misses) and wrongly reconstructed tracks (misreconstruction), as well as for the event selection efficiency including the vertex and enhanced-event selection. In method 1, the correction is performed in two steps. The first step corrects for detector resolution, missed particles and misreconstructed tracks, using an unfolding procedure. The second step corrects for the event selection efficiency. In method 2, the R matrix is constructed in a manner that does not include information on the missed particles and misreconstructed tracks; therefore a correction factor to account for these effects is applied. This correction factor takes into account the missed particles and the misreconstructed tracks, as well as the event selection efficiency. In contrast to method 1, this correction factor is applied as a function of the observable of interest. The reason for this is that the number of missing particles in the reconstruction and the number of misreconstructed tracks both show a dependence on the different observables. The D'Agostini method [54] is used to unfold the detector effects.

The final corrected distributions are obtained by taking the average of two corrected distributions, each corrected using one of the two MC models that describe best the data at detector level. Most of the distributions are best described by PYTHIA8 CUETM1 and EPOS LHC. The only exception is the pseudorapidity distribution of the SD-enhanced event sample, for which PYTHIA8 CUETM1 and PYTHIA8 MBR4C have been used.

6 Systematic uncertainties

The following sources of systematic uncertainty are taken into account: tracking efficiency, description of the pileup modeling, sensitivity to the specific value used for the energy threshold applied to the HF towers, and the dependence on the model used for the corrections.

The systematic uncertainties show almost no dependence on the pseudorapidity of the particles in the fiducial region considered here. For the charged particle multiplicity and p_T distributions, the systematic uncertainties are dependent on the value of the measured observable. The systematic uncertainties associated with the p_T distributions of all charged particles, the leading charged particle, and the integrated spectrum of the latter show a similar behavior.

- Tracking efficiency. The systematic uncertainty due to the difference between the track reconstruction efficiency in data and simulation is $\approx 4\%$. This has been obtained in Ref. [16] at $\sqrt{s} = 8$ TeV and validated for $\sqrt{s} = 13$ TeV

data by comparing the tracking performance of the data set used in this analysis to the performance of the same data set but reconstructed with the (different) tracking conditions used in Ref. [16]. The tracking efficiency is estimated with a data-driven method known as “tag-and-probe” [55] by exploiting resonances decaying into two particles.

- Pileup modeling. The systematic uncertainty associated with the modeling of the pileup contribution is calculated by varying the nominal selection of events with exactly one vertex to that obtained with at least one vertex where only the tracks associated with the vertex with the largest sum of the squared transverse momenta of its tracks are used. The difference between these two selections is taken as the associated uncertainty. For the pseudorapidity distributions, the uncertainty is estimated to be about 1% for the inelastic event sample, while it is about 1.5 and 0.3% for the NSD- and SD-enhanced event samples, respectively. An uncertainty of about 2% on the p_T distributions for the most inclusive selection procedure is obtained, while it is smaller than 1% for the SD-enhanced event sample. The inelastic and NSD-enhanced event samples have similar uncertainties for the multiplicity distributions, first increasing at low multiplicities from 2 to 8% and then decreasing to 0.5% for large multiplicities.
- Event selection with HF. The systematic uncertainty associated with the event selection is determined by varying the threshold applied to the energy of the HF calorimeter towers, while keeping the definition of the stable-particle level unchanged. The default value of the energy threshold applied to the HF calorimeter towers is varied from 5 GeV by ± 1 GeV. In the inelastic and NSD-enhanced event samples an uncertainty of less than 2% for all the relevant distributions is obtained, while for the SD-enhanced sample the uncertainty increases to $\approx 6\%$ for the pseudorapidity distributions and varies between 1 and 15% for the p_T distributions.
- Model dependence. The systematic uncertainty due to the model dependence is calculated as one half of the difference between the corrected distributions using the two MC models mentioned in Sect. 5. For the pseudorapidity distributions, it varies between 0.1 and 1% for the inelastic and NSD-enhanced event samples, and is about 7% for the SD-enhanced sample. For the transverse-momentum distributions, the most inclusive event samples have a maximum uncertainty of about 4% at high p_T , while the SD-enhanced event sample exhibits a maximum uncertainty of 10% around 2 GeV, decreasing at both the low and high ends of the spectrum.

For the event multiplicity distributions, the inelastic and

NSD-enhanced event samples have similar uncertainties with values up to 8%, reaching a maximum uncertainty for low and high multiplicities, and a minimum for multiplicities between 5 and 40.

The total systematic uncertainty is obtained by adding the different sources discussed above in quadrature. Table 2 summarizes all the contributions per observable and per event selection. The total uncertainty is reported for each case.

Due to the statistical limitations of the multiplicity measurement in the SD-enhanced event sample, this distribution is not included in the results.

7 Results

Charged particle distributions corrected to particle level as a function of η , p_T and leading p_T , as well as the integrated leading p_T as a function of $p_{T,\min}$ ($D(p_{T,\min})$), and the multiplicity per event $P(N_{\text{ch}})$ are shown in Fig. 1. They are presented for the different event categories corresponding to the most inclusive (inelastic), the diffraction-depleted (NSD), and the diffraction-enhanced (SD) samples.

The SD-minus and SD-plus samples are mutually exclusive, depending on the side of the forward-detector that contains the hadronic activity. The pseudorapidity distribution of the SD-enhanced event sample is also presented as a symmetrized distribution constructed from the SD-minus and SD-plus enhanced samples and is referred to as the SD-One-Side enhanced event sample. The symmetrization is performed by reflecting the distribution with respect to $\eta = 0$. The pseudorapidity distributions are averaged over the positive and negative η ranges to suppress statistical fluctuations.

The per-event yields, defined in Eq. (1), are obtained experimentally as

$$D(p_{T,\min}) = \frac{1}{N_{\text{events}}} \sum_{p_{T,\text{leading}} > p_{T,\min}} \Delta p_{T,\text{leading}} \left(\frac{d\Delta N}{d\Delta p_{T,\text{leading}}} \right), \quad (2)$$

where N_{events} is the number of events with a leading charged particle, $\Delta p_{T,\text{leading}}$ is the bin width, and ΔN is the number of events with a leading charged particle in each bin.

In general terms, the inelastic and NSD distributions are similar. The pseudorapidity density of the SD-enhanced event sample is about a factor of 4 lower than that of the most inclusive event samples. The p_T distributions (i.e., p_T , leading p_T , and integrated leading p_T) of the SD-enhanced event sample fall very steeply for large p_T values. The charged particle multiplicity distribution of the NSD-enhanced event sample shows a depletion of low-multiplicity events and an

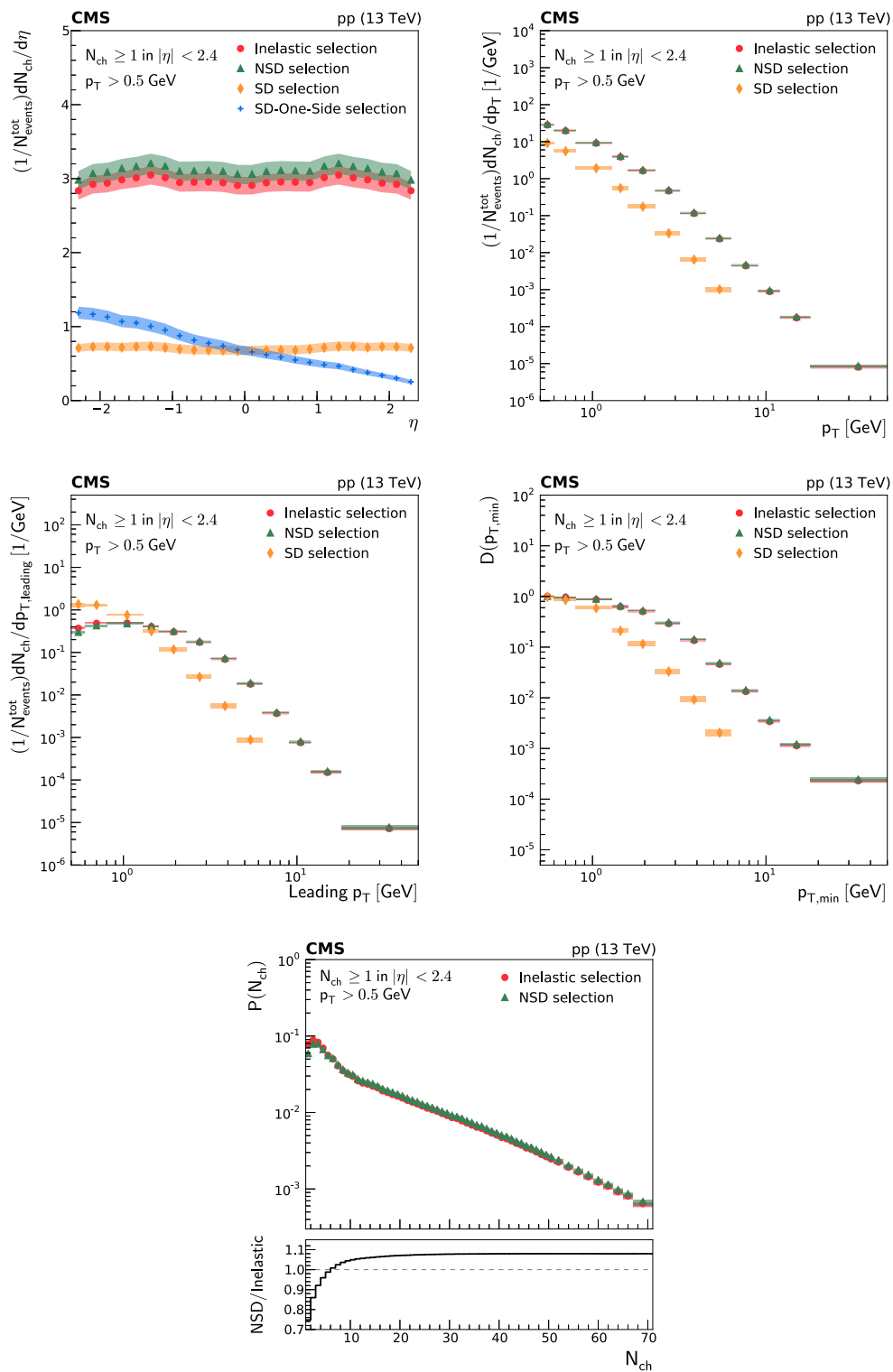


Fig. 1 From top to bottom, left to right: pseudorapidity η , p_T , leading p_T , integrated leading p_T , and multiplicity of charged particles per event for the inelastic (circles), NSD-enhanced (triangles), SD-enhanced (diamonds), and SD-One-Side enhanced (crosses) event samples. The band

encompassing the data points represent the total systematic uncertainty, while the statistical uncertainty is included as a vertical bar for each data point

Table 2 Summary of systematic uncertainties per observable for each of the event samples. The observables are (presented as rows, from top to bottom) pseudorapidity, multiplicity, transverse momentum, leading transverse momentum, and the integral of the latter. The columns, from left to right, represent the following event samples: Inelastic, NSD-enhanced and SD-enhanced. For each observable the respective sources of uncertainty are listed. These are, from top to bottom: the tracking efficiency, the pileup modelling, the event selection and the model dependence. The final value in each case represents the total systematic uncertainty

		Systematic uncertainties (%)		
Observable	Source	Inelastic	NSD-enhanced	SD-enhanced
$\frac{dN_{ch}}{d\eta}$	Tracking efficiency	4	4	4
	Pileup modeling	1	1.6	0.3
	Event selection	< 0.2	1	7
	Model dependence	0.8	0.5	7
	Total	4	4	9
$P(N_{ch})$	Tracking efficiency	4	4	—
	Pileup modeling	0.5–8	0.5–8	—
	Event selection	0–2	0–2	—
	Model dependence	0–8	0–8	—
	Total	4–8	4–8	—
$\frac{dN_{ch}}{d p_T}$	Tracking efficiency	4	4	4
	Pileup modeling	0–2	0.5–2	0–2
	Event selection	< 0.2	1	1–12
	Model dependence	0–4	0–4	4–10
	Total	4	4	7–14
$\frac{dN_{ch}}{d p_{T,leading}}$	Tracking efficiency	4	4	4
	Pileup modeling	0–4	0.5–4	0–4
	Event selection	< 0.2	1	1–12
	Model dependence	0–3	0–3	4–14
	Total	4	4	5–14
$D(p_{T,min})$	Tracking efficiency	4	4	4
	Pileup modeling	0–2	0.5–2	0–2
	Event selection	< 0.2	1	1–12
	Model dependence	0–4	0–4	1–11
	Total	4	4	4–15

increase of high-multiplicity events compared to that of the inelastic sample.

Figure 2 shows the pseudorapidity densities of charged particles for four different event categories. The measurements are compared to the predictions of different MC event generators, namely PYTHIA8 CUETM1, PYTHIA8 MBR4C, and EPOS LHC. The predictions of EPOS LHC provide the best description of the data within uncertainties for the inelastic event sample. The predictions of PYTHIA8 CUETM1 slightly underestimate the measurements, while those of PYTHIA8 MBR4C overestimate them. For the NSD-enhanced event sample, the predictions of EPOS LHC and PYTHIA8 CUETM1 both give a reasonable description of the data within uncertainties, while the predictions of PYTHIA8 MBR4C overestimate the measurements. The opposite behavior is observed for the SD-enhanced event samples, with the predictions of EPOS LHC underestimating the data, and the predictions of PYTHIA8 CUETM1 overestimating them. The predictions from PYTHIA8 MBR4C describe well the SD data within uncertainties, showing only small deviations at the edges of the phase space. The SD-One-Side enhanced event sample is not well described

by EPOS LHC, while PYTHIA8 CUETM1 tends to overestimate data, and the prediction from PYTHIA8 MBR4C describes the measurements within uncertainties over almost the full range, exhibiting some deviations in the regions where the diffractive dissociative system is observed.

Figure 3 shows the charged particle multiplicity distributions for the inelastic and NSD-enhanced event samples. The different event generators provide similar predictions for the inelastic and NSD-enhanced event samples, with differences appearing only at low multiplicities. It is in this low-multiplicity regime that the SD dissociation events contribute the most. The PYTHIA8 MBR4C generator gives the best description of the data in the low-multiplicity region, while PYTHIA8 CUETM1 and EPOS LHC overestimate the data by approximately 20%. This behavior is similar to that observed in the pseudorapidity distribution of the SD-enhanced selection, where PYTHIA8 MBR4C provides the best description of the SD-enhanced event sample. For multiplicities above 35, the predictions of PYTHIA8 CUETM1 give the best description of the data, whereas those of PYTHIA8 MBR4C and EPOS LHC are off by up to 50%. The high multiplicity region is espe-

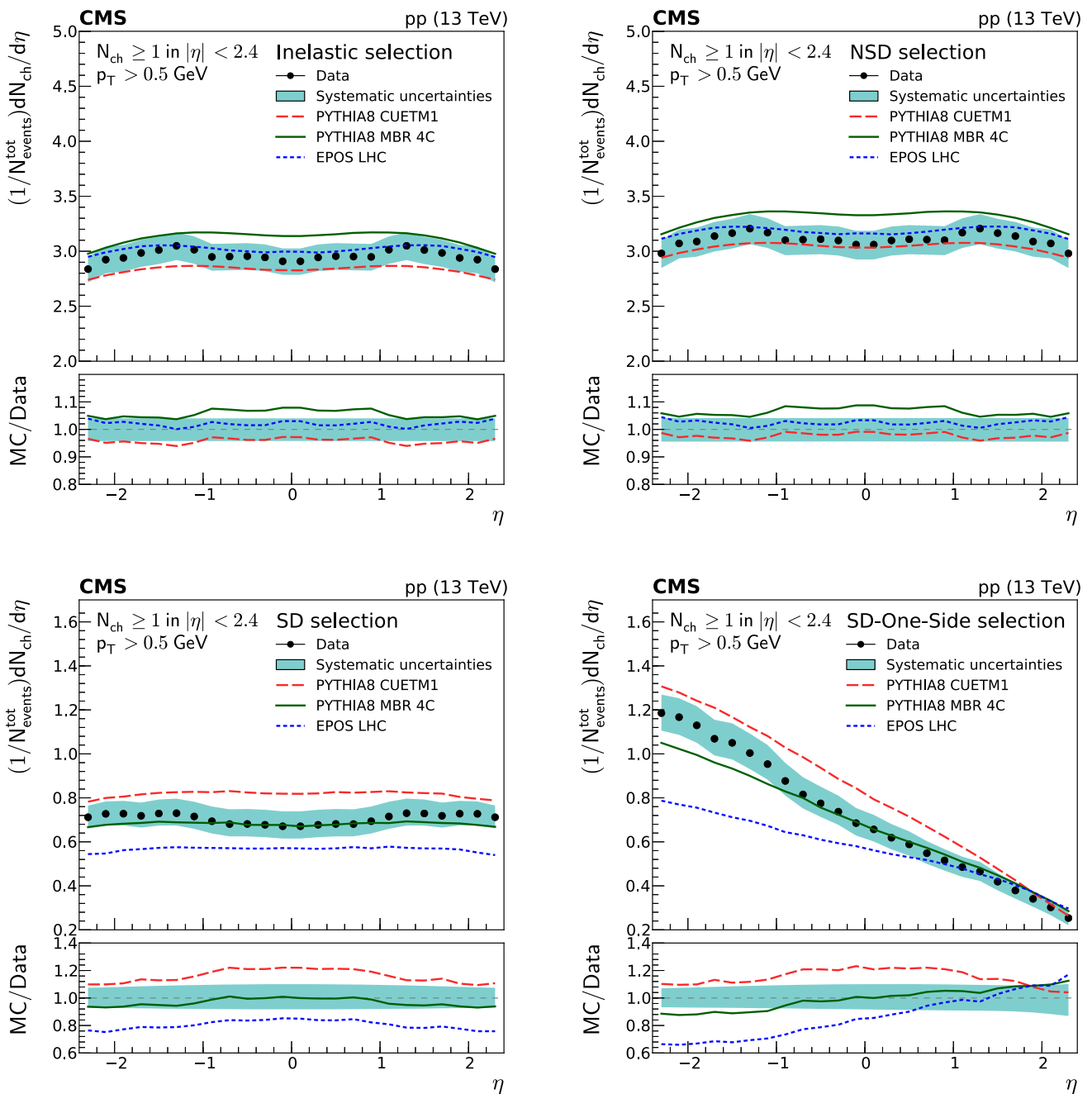


Fig. 2 Charged particle pseudorapidity densities averaged over both positive and negative η ranges. Top to bottom, left to right: inelastic, NSD-, SD-, and SD-One-Side enhanced event samples. The measurements are compared to the predictions of the PYTHIA8 CUETM1 (long dashes), PYTHIA8 MBR4C (continuous line), and EPOS LHC (short

dashes) event generators. The band encompassing the data points represent the total systematic uncertainty, while the statistical uncertainty is included as a vertical bar for each data point. The lower panels show the corresponding MC-to-data ratios

cially sensitive to MPI and improving its modelling could lead to a better understanding of these processes.

Figures 4, 5 and 6 show the charged particle p_T distributions for all the particles, the leading particle, and the integrated spectrum of the latter, for the inelastic, NSD-, and SD-enhanced event samples. The p_T range for the SD-enhanced event sample is smaller compared to the other samples, rang-

ing up to 6.3 GeV instead of 50 GeV. This is a consequence of the more steeply falling p_T spectrum of the SD-enhanced event sample with respect to the other two event categories (Fig. 1).

The p_T distributions of the charged particles in the inelastic and NSD-enhanced event samples are best described by the predictions of PYTHIA8 CUETM1 over almost the full p_T

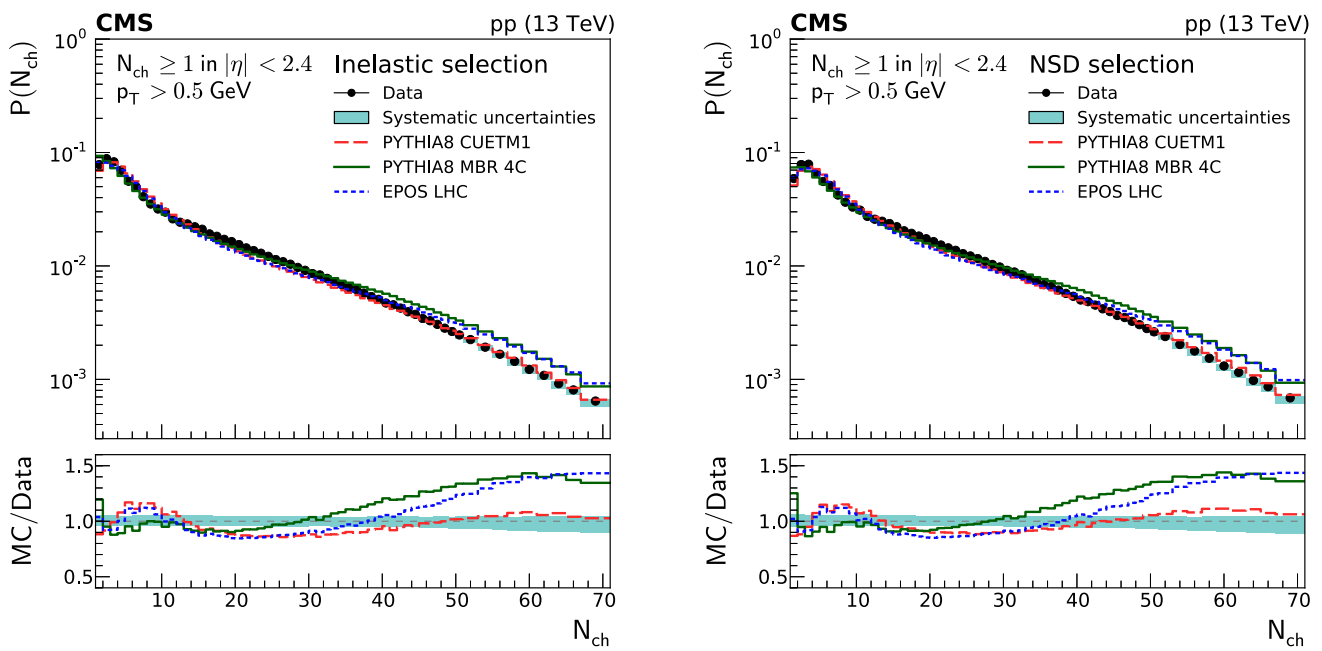


Fig. 3 Charged particle multiplicity distributions of the inelastic (left), and NSD-enhanced (right) event samples. The measurements are compared to the predictions of the PYTHIA8 CUETM1 (long dashes), PYTHIA8 MBR4C (continuous line), and EPOS LHC (short dashes) event genera-

tors. The band encompassing the data points represent the total systematic uncertainty, while the statistical uncertainty is included as a vertical bar for each data point. The lower panels show the corresponding MC-to-data ratios

range. Small deviations of up to 10% in the low- p_T region are observed. This region is dominated by particles coming from MPI. The predictions of PYTHIA8 MBR4C describe the low- p_T region but rapidly start to overestimate particle production for $p_T > 5$ GeV by up to 30%. The predictions of EPOS LHC give a reasonable description of the data for transverse momenta up to $p_T \approx 10$ GeV, while above this value they underestimate it by $\approx 10\%$. In the case of the SD-enhanced event sample, PYTHIA8 CUETM1 gives the best description of the data, while EPOS LHC and PYTHIA8 MBR4C underestimate or overestimate the data by 40 and 80%, respectively. It is interesting to observe how difficult it is to simultaneously describe within a given model both the bulk of soft particles mainly coming from MPI and the high- p_T particles primarily coming from hard parton scattering.

The leading p_T distributions of charged particles and their integral as a function of $p_{T,\min}$ are presented in Figs. 5 and 6, respectively. These two distributions provide valuable information on the modeling of the transition between the non-perturbative and perturbative regimes, and on the modeling of MPI [25]. For the case of the leading transverse momentum distributions, the predictions of EPOS LHC give the best description of the data for the inelastic and NSD-enhanced event samples almost everywhere within the experimental uncertainties with only some small deviations at low- p_T values of up to $\approx 10\%$. For $p_T > 4$ GeV, the predictions of PYTHIA8 CUETM1 are able to reproduce these data. The pre-

dictions of PYTHIA8 MBR4C are not able to describe the data at either low or high p_T for any of the analyzed event samples. In the case of the SD-enhanced event sample, the predictions of PYTHIA8 CUETM1 provide the best description of the data, while those of EPOS LHC disagree by up to $\approx 40\%$.

For the distribution of the integrated leading charged particle p_T as a function of $p_{T,\min}$, the predictions are normalized to the data in the high- $p_{T,\min}$ region, since this region is better described by the models. The $p_{T,\min}$ distribution for the SD-enhanced event sample is very different from the others, and the normalization is performed at $p_{T,\min} = 3.2$ GeV, while for inelastic and NSD-enhanced samples it is performed at $p_{T,\min} = 9$ GeV. The inelastic and NSD-enhanced event samples are best described by the predictions of EPOS LHC and PYTHIA8 CUETM1, although the former overestimates particle production by about 10% at around 4–5 GeV, and the latter underestimates it by a similar amount at around $p_{T,\min} = 1$ GeV. The predictions of PYTHIA8 MBR4C agree with the data in the high- p_T region above 9 GeV but increasingly underestimate the data at lower p_T values, where discrepancies of up to about 20% are observed. The predictions of PYTHIA8 CUETM1 describe best the SD-enhanced data set, while those of EPOS LHC and PYTHIA8 MBR4C overestimate and underestimate the data by up to about 40%, respectively. Comparing the shapes of the $D(p_{T,\min})$ distributions for the inelastic (or NSD-enhanced) and SD-enhanced samples, the transition between the regions dominated by particle produc-

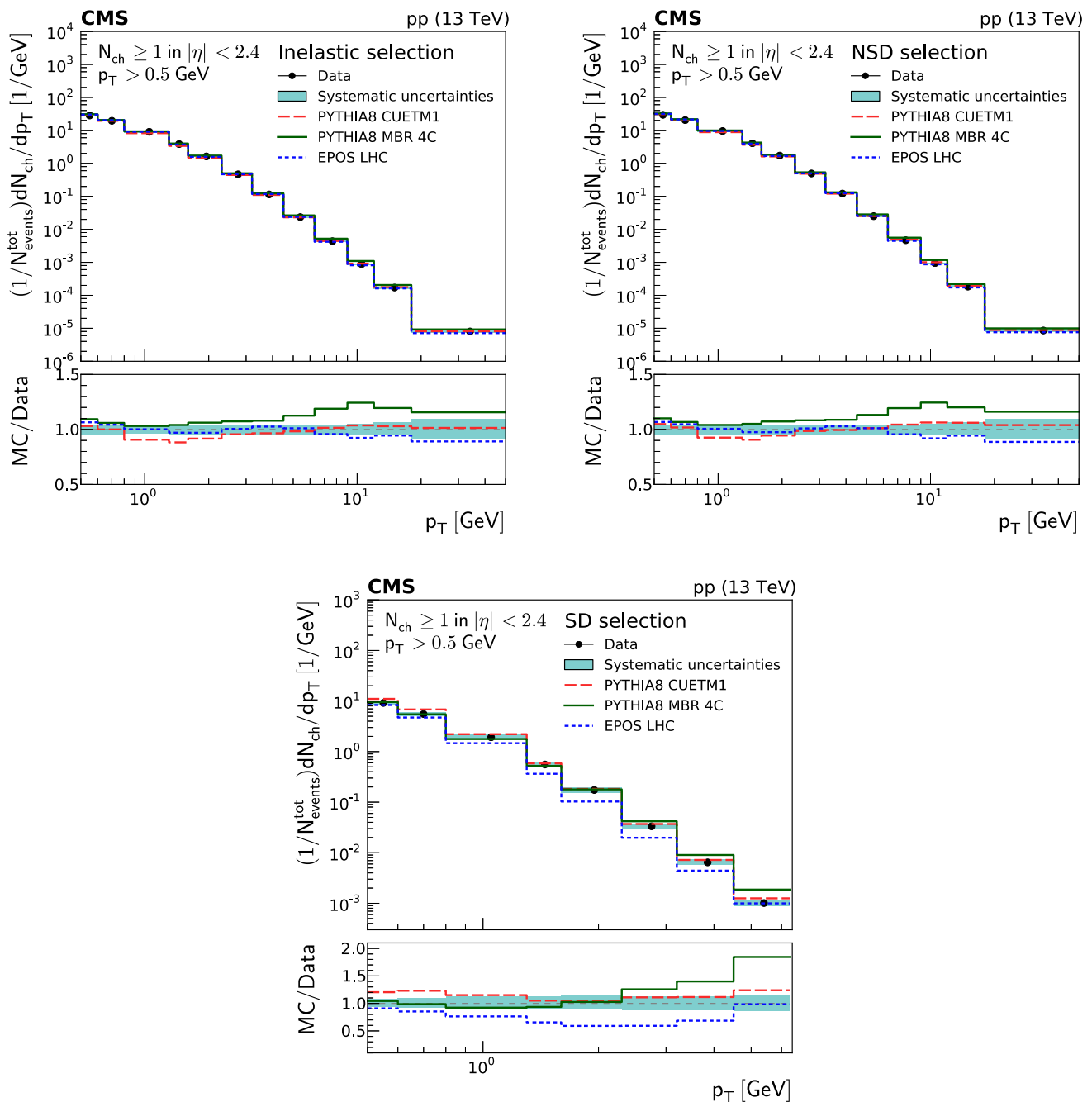


Fig. 4 Charged particle transverse-momentum densities of inelastic (top left), NSD-enhanced (top right), and SD-enhanced (bottom) event samples. The measurements are compared to the predictions of the PYTHIA8 CUETM1 (long dashes), PYTHIA8 MBR4C (continuous line), and

EPOS LHC (short dashes) event generators. The band encompassing the data points represent the total systematic uncertainty, while the statistical uncertainty is included as a vertical bar for each data point. The lower panels show the corresponding MC-to-data ratios

tion from MPIs (and softer diffractive scatterings) and from single-hard parton scatterings seemingly occurs at about 4 and 2 GeV, respectively, as indicated by the (fast) change of slope in the spectra around these $p_{T,min}$ values.

8 Summary

Charged particle distributions measured with the CMS detector in minimum bias proton–proton collisions at a center-of-mass energy of $\sqrt{s} = 13$ TeV have been presented. Charged particles are selected with transverse momenta satisfying

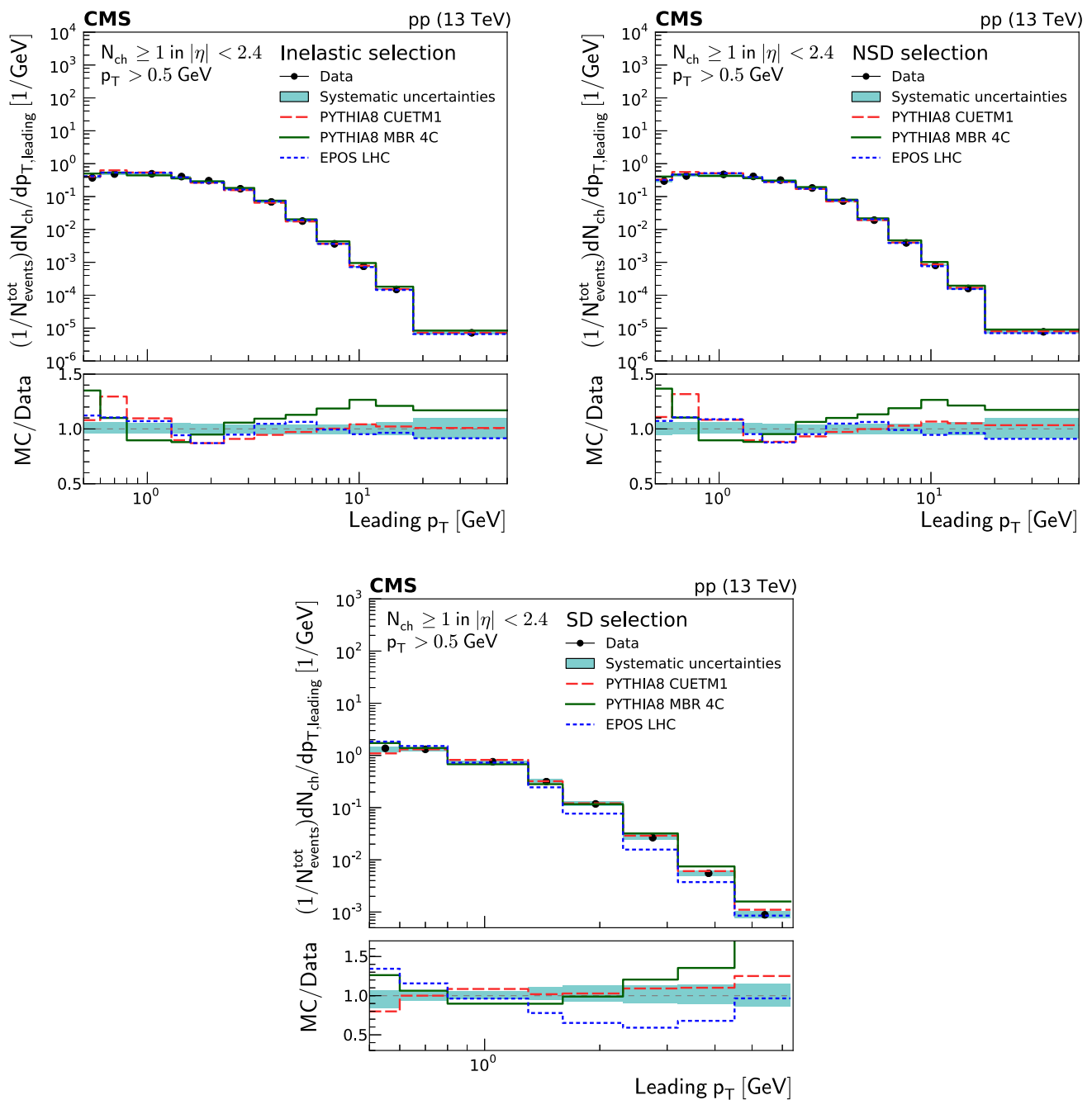


Fig. 5 Leading charged particle p_T distributions of inelastic (top left), NSD-enhanced (top right), and SD-enhanced (bottom) event samples. The measurements are compared to the predictions of the PYTHIA8 CUETM1 (long dashes), PYTHIA8 MBR4C (continuous line), and EPOS

LHC (short dashes) event generators. The band encompassing the data points represent the total systematic uncertainty, while the statistical uncertainty is included as a vertical bar for each data point. The lower panels show the corresponding MC-to-data ratios

$p_T > 0.5 \text{ GeV}$ in the pseudorapidity range $|\eta| < 2.4$. The measured distributions, corrected for detector effects, are presented for three different event samples selected according to the maximum particle energy in the range $3 < |\eta| < 5$. The event samples correspond to an inelastic sample, a sample dominated by nonsingle diffractive dissociation events

(NSD-enhanced sample), and an event sample enriched by single diffractive dissociation events (SD-enhanced sample).

In general, the event generators EPOS LHC, PYTHIA8 CUETM1, and PYTHIA8 MBR4C describe the measurements reasonably well. However, differences are observed in the pseudorapidity distributions for the SD-enhanced event sam-

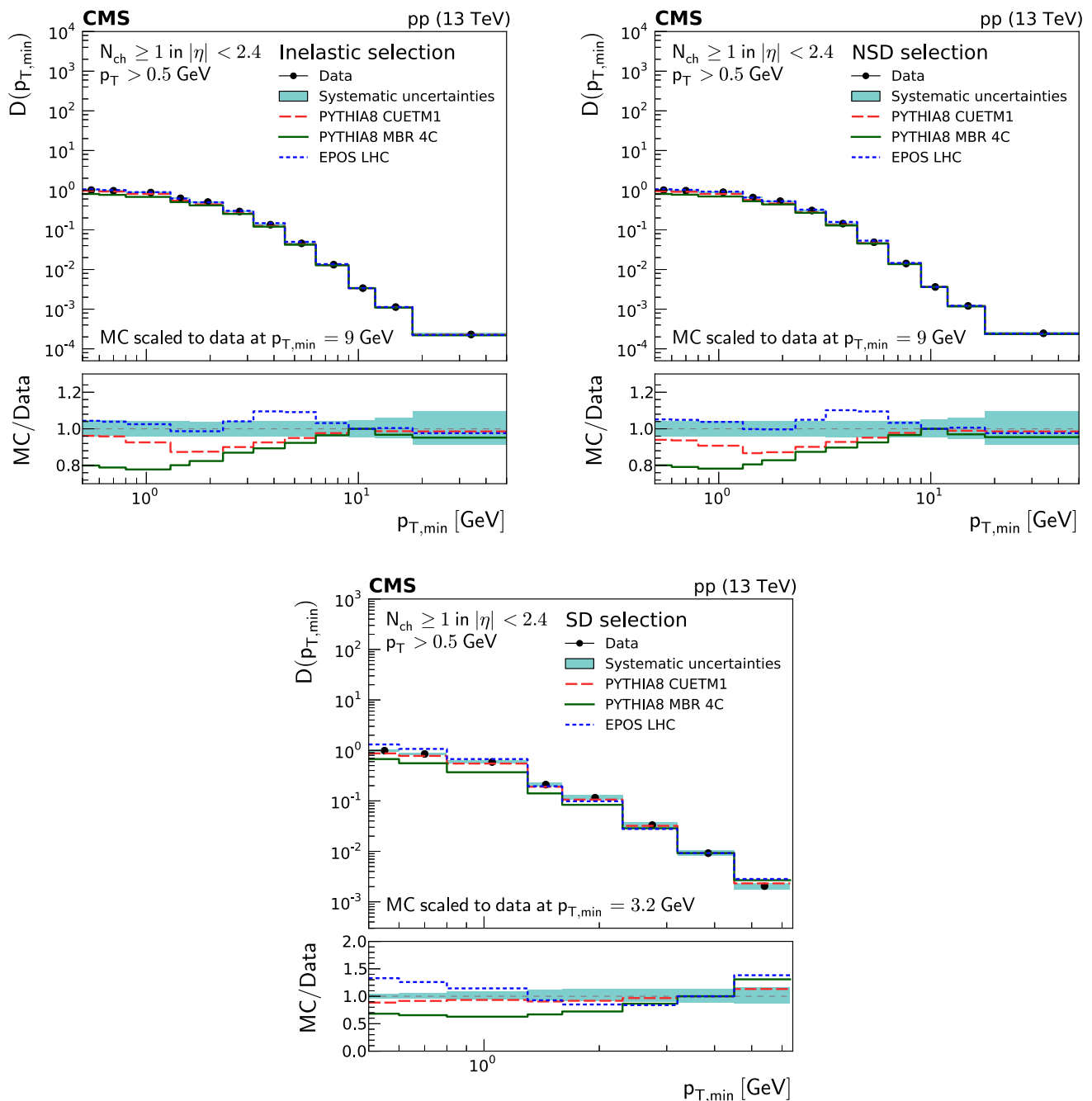


Fig. 6 Integrated leading charged particle p_T distributions as a function of $p_{T,min}$ for inelastic (top left), NSD-enhanced (top right), and SD-enhanced (bottom) event samples. The measurements are compared to the predictions of the PYTHIA8 CUETM1 (long dashes), PYTHIA8 MBR4C (continuous line), and EPOS LHC (short dashes) event generators. The

band encompassing the data points represent the total systematic uncertainty, while the statistical uncertainty is included as a vertical bar for each data point. The lower panels show the corresponding MC-to-data ratios

ple in the region where the diffractive dissociative system is observed. In the distributions integrated over the p_T of the leading particle above a given threshold, $D(p_{T,min})$, deviations of up to 40% are observed in the small p_T region. The change from a relatively flat to a falling $D(p_{T,min})$ distribution occurs at different $p_{T,min}$ values for the diffractive-

enhanced event samples ($p_{T,min} \approx 2$ GeV) and the inelastic and NSD-enhanced sample ($p_{T,min} \approx 4$ GeV).

The level of agreement between these new measurements at $\sqrt{s} = 13$ TeV and the event generators predictions is comparable to that observed for previous measurements at lower energies. The measurements described here provide

new insights into low momentum-exchange parton scatterings that dominate inelastic (including diffractive) pp interactions. The rich variety of distributions presented for different event samples, especially those enhanced in diffractive processes, provide new information to understand the transition from perturbative to nonperturbative regions in particle production in high-energy pp collisions and help constrain model parameters in modern hadronic event generators used in collider and cosmic-ray physics.

Acknowledgements We congratulate our colleagues in the CERN accelerator departments for the excellent performance of the LHC and thank the technical and administrative staffs at CERN and at other CMS institutes for their contributions to the success of the CMS effort. In addition, we gratefully acknowledge the computing centers and personnel of the Worldwide LHC Computing Grid for delivering so effectively the computing infrastructure essential to our analyses. Finally, we acknowledge the enduring support for the construction and operation of the LHC and the CMS detector provided by the following funding agencies: BMWF and FWF (Austria); FNRS and FWO (Belgium); CNPq, CAPES, FAPERJ, and FAPESP (Brazil); MES (Bulgaria); CERN; CAS, MoST, and NSFC (China); COLCIENCIAS (Colombia); MSES and CSF (Croatia); RPF (Cyprus); SENESCYT (Ecuador); MoER, ERC IUT, and ERDF (Estonia); Academy of Finland, MEC, and HIP (Finland); CEA and CNRS/IN2P3 (France); BMBF, DFG, and HGF (Germany); GSRT (Greece); OTKA and NIH (Hungary); DAE and DST (India); IPM (Iran); SFI (Ireland); INFN (Italy); MSIP and NRF (Republic of Korea); LAS (Lithuania); MOE and UM (Malaysia); BUAP, CINVESTAV, CONACYT, LNS, SEP, and UASLP-FAI (Mexico); MBIE (New Zealand); PAEC (Pakistan); MSHE and NSC (Poland); FCT (Portugal); JINR (Dubna); MON, RosAtom, RAS, RFBR and RAEP (Russia); MESTD (Serbia); SEIDI, CPAN, PCTI and FEDER (Spain); Swiss Funding Agencies (Switzerland); MST (Taipei); ThEPcenter, IPST, STAR, and NSTDA (Thailand); TUBITAK and TAEK (Turkey); NASU and SFFR (Ukraine); STFC (United Kingdom); DOE and NSF (USA). Individuals have received support from the Marie-Curie program and the European Research Council and Horizon 2020 Grant, contract No. 675440 (European Union); the Leventis Foundation; the A. P. Sloan Foundation; the Alexander von Humboldt Foundation; the Belgian Federal Science Policy Office; the Fonds pour la Formation à la Recherche dans l'Industrie et dans l'Agriculture (FRIA-Belgium); the Agentschap voor Innovatie door Wetenschap en Technologie (IWT-Belgium); the F.R.S.-FNRS and FWO (Belgium) under the "Excellence of Science - EOS" - be.h project n. 30820817; the Ministry of Education, Youth and Sports (MEYS) of the Czech Republic; the Council of Science and Industrial Research, India; the HOMING PLUS program of the Foundation for Polish Science, cofinanced from European Union, Regional Development Fund, the Mobility Plus program of the Ministry of Science and Higher Education, the National Science Center (Poland), contracts Harmonia 2014/14/M/ST2/00428, Opus 2014/13/B/ST2/02543, 2014/15/B/ST2/03998, and 2015/19/B/ST2/02861, Sonata-bis 2012/07/E/ST2/01406; the National Priorities Research Program by Qatar National Research Fund; the Programa Severo Ochoa del Principado de Asturias; the Thalís and Aristeia programmes cofinanced by EU-ESF and the Greek NSRF; the Rachadapisek Sompot Fund for Postdoctoral Fellowship, Chulalongkorn University and the Chulalongkorn Academic into Its 2nd Century Project Advancement Project (Thailand); the Welch Foundation, contract C-1845; and the Weston Havens Foundation (USA).

Open Access This article is distributed under the terms of the Creative Commons Attribution 4.0 International License (<http://creativecommons.org/licenses/by/4.0/>), which permits unrestricted use, distribution,

and reproduction in any medium, provided you give appropriate credit to the original author(s) and the source, provide a link to the Creative Commons license, and indicate if changes were made. Funded by SCOAP³.

References

1. UA5 Collaboration, Scaling of pseudorapidity distributions at centre-of-mass energies up to 0.9 TeV. *Z. Phys. C* **33**, 1 (1986). <https://doi.org/10.1007/BF01410446>
2. UA4 Collaboration, Pseudorapidity distribution of charged particles in diffraction dissociation events at the CERN SPS collider. *Phys. Lett. B* **166**, 459 (1986) [https://doi.org/10.1016/0370-2693\(86\)91598-4](https://doi.org/10.1016/0370-2693(86)91598-4)
3. UA1 Collaboration, A study of the general characteristics of proton-antiproton collisions at $\sqrt{s} = 0.2$ to 0.9 TeV. *Nucl. Phys. B* **335**, 261 (1990) [https://doi.org/10.1016/0550-3213\(90\)90493-W](https://doi.org/10.1016/0550-3213(90)90493-W)
4. CDF Collaboration, Pseudorapidity distributions of charged particles produced in $p\bar{p}$ interactions at $\sqrt{s} = 630$ GeV and 1800 GeV. *Phys. Rev. D* **41**, 2330 (1990) <https://doi.org/10.1103/PhysRevD.41.2330>
5. CDF Collaboration, Measurement of particle production and inclusive differential cross sections in $p\bar{p}$ collisions at $\sqrt{s} = 1.96$ TeV. *Phys. Rev. D* **79**, 112005 (2009). <https://doi.org/10.1103/PhysRevD.79.112005>. arXiv:0904.1098. [Erratum: DOI10.1103/PhysRevD.82.119903]
6. ALICE Collaboration, Charged-particle multiplicity measurement in proton-proton collisions at $\sqrt{s} = 0.9$ and 2.36 TeV with ALICE at LHC. *Eur. Phys. J. C* **68**, 89 (2010). <https://doi.org/10.1140/epjcs/10052-010-1339-x>. arXiv:1004.3034
7. ALICE Collaboration, Charged-particle multiplicity measurement in proton-proton collisions at $\sqrt{s} = 7$ TeV with ALICE at LHC. *Eur. Phys. J. C* **68**, 345 (2010). <https://doi.org/10.1140/epjcs/10052-010-1350-2>. arXiv:1004.3514
8. ALICE Collaboration, Charged-particle multiplicities in proton-proton collisions at $\sqrt{s} = 0.9$ to 8 TeV. *Eur. Phys. J. C* **77**, 33 (2017). <https://doi.org/10.1140/epjcs/10052-016-4571-1>. arXiv:1509.07541
9. ALICE Collaboration, Charged-particle multiplicity distributions over a wide pseudorapidity range in proton-proton collisions at $\sqrt{s} = 0.9, 7$, and 8 TeV. *Eur. Phys. J. C* **77**, 852 (2017). <https://doi.org/10.1140/epjcs/10052-017-5412-6>. arXiv:1708.01435
10. ATLAS Collaboration, Charged-particle multiplicities in pp interactions at $\sqrt{s} = 900$ GeV measured with the ATLAS detector at the LHC. *Phys. Lett. B* **688**, 21 (2010). <https://doi.org/10.1016/j.physletb.2010.03.064>. arXiv:1003.3124
11. ATLAS Collaboration, Charged-particle multiplicities in pp interactions measured with the ATLAS detector at the LHC. *New J. Phys.* **13**, 053033 (2011). <https://doi.org/10.1088/1367-2630/13/5/053033>. arXiv:1012.5104
12. ATLAS Collaboration, Charged-particle distributions in pp interactions at $\sqrt{s} = 8$ TeV measured with the ATLAS detector. *Eur. Phys. J. C* **76**, 403 (2016). <https://doi.org/10.1140/epjcs/10052-016-4203-9>. arXiv:1603.02439
13. CMS Collaboration, Transverse momentum and pseudorapidity distributions of charged hadrons in pp collisions at $\sqrt{s} = 0.9$ and 2.36 TeV. *JHEP* **02**, 041 (2010). [https://doi.org/10.1007/JHEP02\(2010\)041](https://doi.org/10.1007/JHEP02(2010)041). arXiv:1002.0621
14. CMS Collaboration, Transverse-momentum and pseudorapidity distributions of charged hadrons in pp collisions at $\sqrt{s} = 7$ TeV. *Phys. Rev. Lett.* **105**, 022002 (2010). <https://doi.org/10.1103/PhysRevLett.105.022002>. arXiv:1005.3299

15. CMS Collaboration, Charged particle multiplicities in pp interactions at $\sqrt{s} = 0.9, 2.36, \text{ and } 7 \text{ TeV}$. JHEP **01**, 079 (2011). [https://doi.org/10.1007/JHEP01\(2011\)079](https://doi.org/10.1007/JHEP01(2011)079). arXiv:1011.5531
16. CMS, TOTEM Collaboration, Measurement of pseudorapidity distributions of charged particles in proton–proton collisions at $\sqrt{s} = 8 \text{ TeV}$ by the CMS and TOTEM experiments. Eur. Phys. J. C **74**, 3053 (2014). <https://doi.org/10.1140/epjc/s10052-014-3053-6>. arXiv:1405.0722
17. CMS Collaboration, Production of leading charged particles and leading charged-particle jets at small transverse momenta in pp collisions at $\sqrt{s} = 8 \text{ TeV}$. Phys. Rev. D **92**, 112001 (2015). <https://doi.org/10.1103/PhysRevD.92.112001>. arXiv:1507.00233
18. LHCb Collaboration, Measurement of charged particle multiplicities in pp collisions at $\sqrt{s} = 7 \text{ TeV}$ in the forward region. Eur. Phys. J. C **72**, 1947 (2012). <https://doi.org/10.1140/epjc/s10052-012-1947-8>. arXiv:1112.4592
19. TOTEM Collaboration, Measurement of the forward charged particle pseudorapidity density in pp collisions at $\sqrt{s} = 7 \text{ TeV}$ with the TOTEM experiment. Europhys. Lett. **98**, 31002 (2012). <https://doi.org/10.1209/0295-5075/98/31002>. arXiv:1205.4105
20. CMS Collaboration, Event generator tunes obtained from underlying event and multiparton scattering measurements. Eur. Phys. J. C **76**, 155 (2016). <https://doi.org/10.1140/epjc/s10052-016-3988-x>. arXiv:1512.00815
21. ALICE Collaboration, Pseudorapidity and transverse-momentum distributions of charged particles in proton-proton collisions at $\sqrt{s} = 13 \text{ TeV}$. Phys. Lett. B **753**, 319 (2016). <https://doi.org/10.1016/j.physletb.2015.12.030>. arXiv:1509.08734
22. ATLAS Collaboration, Charged-particle distributions in $\sqrt{s} = 13 \text{ TeV}$ pp interactions measured with the ATLAS detector at the LHC. Phys. Lett. B **758**, 67 (2016). <https://doi.org/10.1016/j.physletb.2016.04.050>. arXiv:1602.01633
23. ATLAS Collaboration, Charged-particle distributions at low transverse momentum in $\sqrt{s} = 13 \text{ TeV}$ pp interactions measured with the ATLAS detector at the LHC. Eur. Phys. J. C **76**, 502 (2016). <https://doi.org/10.1140/epjc/s10052-016-4335-y>. arXiv:1606.01133
24. CMS Collaboration, Pseudorapidity distribution of charged hadrons in proton-proton collisions at $\sqrt{s} = 13 \text{ TeV}$. Phys. Lett. B **751**, 143 (2015). <https://doi.org/10.1016/j.physletb.2015.10.004>. arXiv:1507.05915
25. A. Grebenyuk et al., Jet production and the inelastic pp cross section at the LHC. Phys. Rev. D **86**, 117501 (2012). <https://doi.org/10.1103/PhysRevD.86.117501>. arXiv:1209.6265
26. CMS Collaboration, Description and performance of track and primary-vertex reconstruction with the CMS tracker. JINST **9**, P10009 (2014). <https://doi.org/10.1088/1748-0221/9/10/P10009>. arXiv:1405.6569
27. CMS Collaboration, The CMS experiment at the CERN LHC. JINST **3**, S08004 (2008). <https://doi.org/10.1088/1748-0221/3/08/S08004>
28. T. Sjöstrand, S. Mrenna, P. Skands, A brief introduction to PYTHIA 8.1. Comput. Phys. Commun. **178**, 852 (2008). <https://doi.org/10.1016/j.cpc.2008.01.036>. arXiv:0710.3820
29. P.Z. Skands, D. Wicke, Non-perturbative QCD effects and the top mass at the Tevatron. Eur. Phys. J. C **52**, 133 (2007). <https://doi.org/10.1140/epjc/s10052-007-0352-1>. arXiv:hep-ph/0703081
30. V.N. Gribov, L.N. Lipatov, Deep inelastic e p scattering in perturbation theory. Sov. J. Nucl. Phys. **15**, 438 (1972). [*Yad. Fiz.* **15** (1972) 781]
31. G. Altarelli, G. Parisi, Asymptotic freedom in parton language. Nucl. Phys. B **126**, 298 (1977). [https://doi.org/10.1016/0550-3213\(77\)90384-4](https://doi.org/10.1016/0550-3213(77)90384-4)
32. Y.L. Dokshitzer, Calculation of the structure functions for deep inelastic scattering and e^+e^- annihilation by perturbation theory in quantum chromodynamics. Sov. Phys. JETP **46**, 641 (1977). [*Zh. Eksp. Teor. Fiz.* **73** (1977) 1216]
33. B. Andersson, G. Gustafson, G. Ingelman, T. Sjöstrand, Parton fragmentation and string dynamics. Phys. Rept. **97**, 31 (1983). [https://doi.org/10.1016/0370-1573\(83\)90080-7](https://doi.org/10.1016/0370-1573(83)90080-7)
34. G.A. Schuler, T. Sjöstrand, Hadronic diffractive cross sections and the rise of the total cross section. Phys. Rev. D **49**, 2257 (1994). <https://doi.org/10.1103/PhysRevD.49.2257>
35. H1 Collaboration, Measurement and QCD analysis of the diffractive deep-inelastic scattering cross-section at HERA. Eur. Phys. J. C **48**, 715 (2006). <https://doi.org/10.1140/epjc/s10052-006-0035-3>. arXiv:hep-ex/0606004
36. H1 Collaboration, Dijet cross sections and parton densities in diffractive DIS at HERA. JHEP **10**, 042 (2007). <https://doi.org/10.1088/1126-6708/2007/10/042>. arXiv:0708.3217
37. P. Newman, M. Wing, The hadronic final state at HERA. Rev. Mod. Phys. **86**, 1037 (2014). <https://doi.org/10.1103/RevModPhys.86.1037>. arXiv:1308.3368
38. P. Skands, S. Carrazza, J. Rojo, Tuning PYTHIA 8.1: the Monash 2013 Tune. Eur. Phys. J. C **74**, 3024 (2014). <https://doi.org/10.1140/epjc/s10052-014-3024-y>. arXiv:1404.5630
39. NNPDF Collaboration, Unbiased global determination of parton distributions and their uncertainties at NNLO and at LO. Nucl. Phys. B **855**, 153 (2012). <https://doi.org/10.1016/j.nuclphysb.2011.09.024>. arXiv:1107.2652
40. NNPDF Collaboration, Parton distributions with QED corrections. Nucl. Phys. B **877**, 290 (2013). <https://doi.org/10.1016/j.nuclphysb.2013.10.010>. arXiv:1308.0598
41. R. Ciesielski, K. Goulianos, MBR Monte Carlo simulation in PYTHIA8. PoS ICHEP2012, 301 (2013). <https://doi.org/10.22323/1.174.0301>. arXiv:1205.1446
42. R. Corke, T. Sjöstrand, Interleaved parton showers and tuning prospects. JHEP **03**, 032 (2011). [https://doi.org/10.1007/JHEP03\(2011\)032](https://doi.org/10.1007/JHEP03(2011)032). arXiv:1011.1759
43. K.A. Goulianos, Diffraction in QCD. in *Corfu Summer Institute on Elementary Particle Physics (Corfu 2001) Corfu, Greece, August 31–September 20, 2001*. (2002). arXiv:hep-ph/0203141
44. K.A. Goulianos, Hadronic diffraction: Where do we stand?. in *Results and perspectives in particle physics. Proceedings, 18th Rencontres de Physique de la Vallée d'Aoste, La Thuile, Italy, February 29–March 6, 2004*, p. 251. (2004). arXiv:hep-ph/0407035
45. CMS Collaboration, Measurement of diffraction dissociation cross sections in pp collisions at $\sqrt{s} = 7 \text{ TeV}$. Phys. Rev. D **92**, 012003 (2015). <https://doi.org/10.1103/PhysRevD.92.012003>. arXiv:1503.08689
46. K. Werner, F.M. Liu, T. Pierog, Parton ladder splitting and the rapidity dependence of transverse momentum spectra in deuteron-gold collisions at rhic. Phys. Rev. C **74**, 044902 (2006). <https://doi.org/10.1103/PhysRevC.74.044902>. arXiv:hep-ph/0506232
47. D. d'Enterria, R. Engel, T. Pierog, S. Ostapchenko, K. Werner, Constraints from the first lhc data on hadronic event generators for ultra-high energy cosmic-ray physics. Astropart. Phys. **35**, 98 (2011). <https://doi.org/10.1016/j.astropartphys.2011.05.002>. arXiv:1101.5596
48. V.N. Gribov, A reggeon diagram technique. Sov. Phys. JETP **26**, 414 (1968). [*Zh. Eksp. Teor. Fiz.* **53** (1967) 654]
49. T. Pierog, EPOS LHC: test of collective hadronization with data measured at the CERN Large Hadron Collider. Phys. Rev. C **92**, 034906 (2015). <https://doi.org/10.1103/PhysRevC.92.034906>. arXiv:1306.0121
50. T. Pierog, LHC results and high energy cosmic ray interaction models. J. Phys. Conf. Ser. **409**, 012008 (2013). <https://doi.org/10.1088/1742-6596/409/1/012008>
51. GEANT4 Collaboration, GEANT4—a simulation toolkit. Nucl. Instrum. Meth. A **506**, 250 (2003). [https://doi.org/10.1016/S0168-9002\(03\)01368-8](https://doi.org/10.1016/S0168-9002(03)01368-8)

52. CMS Collaboration, Measurement of long-range near-side two-particle angular correlations in pp collisions at $\sqrt{s} = 13$ TeV. *Phys. Rev. Lett.* **116**, 172302 (2015). <https://doi.org/10.1103/PhysRevLett.116.172302>. arXiv:1510.03068
53. CMS Collaboration, Track and vertex reconstruction in CMS. *Nucl. Inst. Meth. A* **582**, 781 (2007). <https://doi.org/10.1016/j.nima.2007.07.091>
54. G. D'Agostini, A multidimensional unfolding method based on Bayes' theorem. *Nucl. Instrum. Methods A* **362**, 487 (1995). [https://doi.org/10.1016/0168-9002\(95\)00274-X](https://doi.org/10.1016/0168-9002(95)00274-X)
55. CMS Collaboration, Measurement of the inclusive W and Z production cross sections in pp collisions at $\sqrt{s} = 7$ TeV. *JHEP* **10**, 132 (2011). [https://doi.org/10.1007/JHEP10\(2011\)132](https://doi.org/10.1007/JHEP10(2011)132). arXiv:1107.4789

CMS Collaboration

Yerevan Physics Institute, Yerevan, Armenia

A. M. Sirunyan, A. Tumasyan

Institut für Hochenergiephysik, Wien, Austria

W. Adam, F. Ambroggi, E. Asilar, T. Bergauer, J. Brandstetter, E. Brondolin, M. Dragicevic, J. Erö, A. Escalante Del Valle, M. Flechl, R. Frühwirth¹, V. M. Ghete, J. Hrubec, M. Jeitler¹, N. Krammer, I. Krätschmer, D. Liko, T. Madlener, I. Mikulec, N. Rad, H. Rohringer, J. Schieck¹, R. Schöfbeck, M. Spanring, D. Spitzbart, A. Taurok, W. Waltenberger, J. Wittmann, C.-E. Wulz¹, M. Zarucki

Institute for Nuclear Problems, Minsk, Belarus

V. Chekhovsky, V. Mossolov, J. Suarez Gonzalez

Universiteit Antwerpen, Antwerpen, Belgium

E. A. De Wolf, D. Di Croce, X. Janssen, J. Lauwers, M. Pieters, M. Van De Klundert, H. Van Haevermaet, P. Van Mechelen, N. Van Remortel

Vrije Universiteit Brussel, Brussel, Belgium

S. Abu Zeid, F. Blekman, J. D'Hondt, I. De Bruyn, J. De Clercq, K. Deroover, G. Flouris, D. Lontkovskiy, S. Lowette, I. Marchesini, S. Moortgat, L. Moreels, Q. Python, K. Skovpen, S. Tavernier, W. Van Doninck, P. Van Mulders, I. Van Parijs

Université Libre de Bruxelles, Brussels, Belgium

D. Beghin, B. Bilin, H. Brun, B. Clerbaux, G. De Lentdecker, H. Delannoy, B. Dorney, G. Fasanella, L. Favart, R. Goldouzian, A. Grebenyuk, A. K. Kalsi, T. Lenzi, J. Luetic, N. Postiau, E. Starling, L. Thomas, C. Vander Velde, P. Vanlaer, D. Vannerom, Q. Wang

Ghent University, Ghent, Belgium

T. Cornelis, D. Dobur, A. Fagot, M. Gul, I. Khvastunov², D. Poyraz, C. Roskas, D. Trocino, M. Tytgat, W. Verbeke, B. Vermassen, M. Vit, N. Zaganidis

Université Catholique de Louvain, Louvain-la-Neuve, Belgium

H. Bakhshiansohi, O. Bondu, S. Brochet, G. Bruno, C. Caputo, P. David, C. Delaere, M. Delcourt, B. Francois, A. Giammanco, G. Krintiras, V. Lemaître, A. Magitteri, A. Mertens, M. Musich, K. Piotrkowski, A. Saggio, M. Vidal Marono, S. Wertz, J. Zobec

Centro Brasileiro de Pesquisas Físicas, Rio de Janeiro, Brazil

F. L. Alves, G. A. Alves, L. Brito, G. Correia Silva, C. Hensel, A. Moraes, M. E. Pol, P. Rebello Teles

Universidade do Estado do Rio de Janeiro, Rio de Janeiro, Brazil

E. Belchior Batista Das Chagas, W. Carvalho, J. Chinellato³, E. Coelho, E. M. Da Costa, G. G. Da Silveira⁴, D. De Jesus Damiao, C. De Oliveira Martins, S. Fonseca De Souza, H. Malbouisson, D. Matos Figueiredo, M. Melo De Almeida, C. Mora Herrera, L. Mundim, H. Nogima, W. L. Prado Da Silva, L. J. Sanchez Rosas, A. Santoro, A. Sznajder, M. Thiel, E. J. Tonelli Manganote³, F. Torres Da Silva De Araujo, A. Vilela Pereira

Universidade Estadual Paulista^a, Universidade Federal do ABC^b, São Paulo, Brazil

S. Ahuja^a, C. A. Bernardes^a, L. Calligaris^a, T. R. Fernandez Perez Tomei^a, E. M. Gregores^b, P. G. Mercadante^b, S. F. Novaes^a, Sandra S. Padula^a, D. Romero Abad^b

Institute for Nuclear Research and Nuclear Energy, Bulgarian Academy of Sciences, Sofia, Bulgaria

A. Aleksandrov, R. Hadjiiska, P. Iaydjiev, A. Marinov, M. Misheva, M. Rodozov, M. Shopova, G. Sultanov

University of Sofia, Sofia, Bulgaria

A. Dimitrov, L. Litov, B. Pavlov, P. Petkov

Beihang University, Beijing, China

W. Fang⁵, X. Gao⁵, L. Yuan

Institute of High Energy Physics, Beijing, China

M. Ahmad, J. G. Bian, G. M. Chen, H. S. Chen, M. Chen, Y. Chen, C. H. Jiang, D. Leggat, H. Liao, Z. Liu, F. Romeo, S. M. Shaheen, A. Spiezia, J. Tao, C. Wang, Z. Wang, E. Yazgan, H. Zhang, J. Zhao

State Key Laboratory of Nuclear Physics and Technology, Peking University, Beijing, China

Y. Ban, G. Chen, J. Li, L. Li, Q. Li, Y. Mao, S. J. Qian, D. Wang, Z. Xu

Tsinghua University, Beijing, China

Y. Wang

Universidad de Los Andes, Bogotá, Colombia

C. Avila, A. Cabrera, C. A. Carrillo Montoya, L. F. Chaparro Sierra, C. Florez, C. F. González Hernández, M. A. Segura Delgado

University of Split, Faculty of Electrical Engineering, Mechanical Engineering and Naval Architecture, Split, Croatia

B. Courbon, N. Godinovic, D. Lelas, I. Puljak, T. Sculac

University of Split, Faculty of Science, Split, Croatia

Z. Antunovic, M. Kovac

Institute Rudjer Boskovic, Zagreb, Croatia

V. Brigljevic, D. Ferencek, K. Kadija, B. Mesic, A. Starodumov⁶, T. Susa

University of Cyprus, Nicosia, Cyprus

M. W. Ather, A. Attikis, G. Mavromanolakis, J. Mousa, C. Nicolaou, F. Ptochos, P. A. Razis, H. Rykaczewski

Charles University, Prague, Czech Republic

M. Finger⁷, M. Finger Jr.⁷

Escuela Politécnica Nacional, Quito, Ecuador

E. Ayala

Universidad San Francisco de Quito, Quito, Ecuador

E. Carrera Jarrin

Academy of Scientific Research and Technology of the Arab Republic of Egypt, Egyptian Network of High Energy Physics, Cairo, Egypt

M. A. Mahmoud^{8,9}, Y. Mohammed⁸, E. Salama^{9,10}

National Institute of Chemical Physics and Biophysics, Tallinn, Estonia

S. Bhowmik, A. Carvalho Antunes De Oliveira, R. K. Dewanjee, K. Ehataht, M. Kadastik, M. Raidal, C. Veelken

Department of Physics, University of Helsinki, Helsinki, Finland

P. Eerola, H. Kirschenmann, J. Pekkanen, M. Voutilainen

Helsinki Institute of Physics, Helsinki, Finland

J. Havukainen, J. K. Heikkilä, T. Järvinen, V. Karimäki, R. Kinnunen, T. Lampén, K. Lassila-Perini, S. Laurila, S. Lehti, T. Lindén, P. Luukka, T. Mäenpää, H. Siikonen, E. Tuominen, J. Tuominiemi

Lappeenranta University of Technology, Lappeenranta, Finland

T. Tuuva

IRFU, CEA, Université Paris-Saclay, Gif-sur-Yvette, France

M. Besancon, F. Couderc, M. Dejardin, D. Denegri, J. L. Faure, F. Ferri, S. Ganjour, A. Givernaud, P. Gras,

G. Hamel de Monchenault, P. Jarry, C. Leloup, E. Locci, J. Malcles, G. Negro, J. Rander, A. Rosowsky, M. Ö. Sahin, M. Titov

Laboratoire Leprince-Ringuet, Ecole polytechnique, CNRS/IN2P3, Université Paris-Saclay, Palaiseau, France

A. Abdulsalam¹¹, C. Amendola, I. Antropov, F. Beaudette, P. Busson, C. Charlot, R. Granier de Cassagnac, I. Kucher, S. Lisniak, A. Lobanov, J. Martin Blanco, M. Nguyen, C. Ochando, G. Ortona, P. Paganini, P. Pigard, R. Salerno, J. B. Sauvan, Y. Sirois, A. G. Stahl Leiton, A. Zabi, A. Zghiche

Université de Strasbourg, CNRS, IPHC UMR 7178, 67000 Strasbourg, France

J.-L. Agram¹², J. Andrea, D. Bloch, J.-M. Brom, E. C. Chabert, V. Cherepanov, C. Collard, E. Conte¹², J.-C. Fontaine¹², D. Gelé, U. Goerlach, M. Jansová, A.-C. Le Bihan, N. Tonon, P. Van Hove

Centre de Calcul de l'Institut National de Physique Nucleaire et de Physique des Particules, CNRS/IN2P3, Villeurbanne, France

S. Gadrat

Université de Lyon, Université Claude Bernard Lyon 1, CNRS-IN2P3, Institut de Physique Nucléaire de Lyon, Villeurbanne, France

S. Beauceron, C. Bernet, G. Boudoul, N. Chanon, R. Chierici, D. Contardo, P. Depasse, H. El Mamouni, J. Fay, L. Finco, S. Gascon, M. Gouzevitch, G. Grenier, B. Ille, F. Lagarde, I. B. Laktineh, H. Lattaud, M. Lethuillier, L. Mirabito, A. L. Pequegnot, S. Perries, A. Popov¹³, V. Sordini, M. Vander Donckt, S. Viret, S. Zhang

Georgian Technical University, Tbilisi, Georgia

A. Khvedelidze⁷

Tbilisi State University, Tbilisi, Georgia

Z. Tsamalaidze⁷

RWTH Aachen University, I. Physikalisches Institut, Aachen, Germany

C. Autermann, L. Feld, M. K. Kiesel, K. Klein, M. Lipinski, M. Preuten, M. P. Rauch, C. Schomakers, J. Schulz, M. Teroerde, B. Wittmer, V. Zhukov¹³

RWTH Aachen University, III. Physikalisches Institut A, Aachen, Germany

A. Albert, D. Duchardt, M. Endres, M. Erdmann, T. Esch, R. Fischer, S. Ghosh, A. Güth, T. Hebbeker, C. Heidemann, K. Hoepfner, H. Keller, S. Knutzen, L. Mastrolorenzo, M. Merschmeyer, A. Meyer, P. Millet, S. Mukherjee, T. Pook, M. Radziej, H. Reithler, M. Rieger, F. Scheuch, A. Schmidt, D. Teysier

RWTH Aachen University, III. Physikalisches Institut B, Aachen, Germany

G. Flügge, O. Hlushchenko, B. Kargoll, T. Kress, A. Künsken, T. Müller, A. Nehr Korn, A. Nowack, C. Pistone, O. Pooth, H. Sert, A. Stahl¹⁴

Deutsches Elektronen-Synchrotron, Hamburg, Germany

M. Aldaya Martin, T. Arndt, C. Asawatangtrakuldee, I. Babounikau, K. Beernaert, O. Behnke, U. Behrens, A. Bermúdez Martínez, D. Bertsche, A. A. Bin Anuar, K. Borras¹⁵, V. Botta, A. Campbell, P. Connor, C. Contreras-Campana, F. Costanza, V. Danilov, A. De Wit, M. M. Defranchis, C. Diez Pardos, D. Domínguez Damiani, G. Eckerlin, T. Eichhorn, A. Elwood, E. Eren, E. Gallo¹⁶, A. Geiser, J. M. Grados Luyando, A. Grohsjean, P. Gunnellini, M. Guthoff, A. Harb, J. Hauk, H. Jung, M. Kasemann, J. Keaveney, C. Kleinwort, J. Knolle, D. Krücker, W. Lange, A. Lelek, T. Lenz, K. Lipka, W. Lohmann¹⁷, R. Mankel, I.-A. Melzer-Pellmann, A. B. Meyer, M. Meyer, M. Missiroli, G. Mittag, J. Mnich, V. Myronenko, S. K. Pflitsch, D. Pitzl, A. Raspereza, M. Savitskyi, P. Saxena, P. Schütze, C. Schwanenberger, R. Shevchenko, A. Singh, N. Stefaniuk, H. Tholen, A. Vagnerini, G. P. Van Onsem, R. Walsh, Y. Wen, K. Wichmann, C. Wissing, O. Zenaiev

University of Hamburg, Hamburg, Germany

R. Aggleton, S. Bein, A. Benecke, V. Blobel, M. Centis Vignali, T. Dreyer, E. Garutti, D. Gonzalez, J. Haller, A. Hinzmann, M. Hoffmann, A. Karavdina, G. Kasieczka, R. Klanner, R. Kogler, N. Kovalchuk, S. Kurz, V. Kutzner, J. Lange, D. Marconi, J. Multhaup, M. Niedziela, D. Nowatschin, A. Perieanu, A. Reimers, O. Rieger, C. Scharf, P. Schleper, S. Schumann, J. Schwandt, J. Sonneveld, H. Stadie, G. Steinbrück, F. M. Stober, M. Stöver, D. Troendle, E. Usai, A. Vanhoefer, B. Vormwald

Karlsruher Institut fuer Technology, Karlsruhe, Germany

M. Akbiyik, C. Barth, M. Baselga, S. Baur, E. Butz, R. Caspart, T. Chwalek, F. Colombo, W. De Boer, A. Dierlamm, N. Faltermann, B. Freund, M. Giffels, M. A. Harrendorf, F. Hartmann¹⁴, S. M. Heindl, U. Husemann, F. Kassel¹⁴, I. Katkov¹³, S. Kudella, H. Mildner, S. Mitra, M. U. Mozer, Th. Müller, M. Plagge, G. Quast, K. Rabbertz, M. Schröder, I. Shvetsov, G. Sieber, H. J. Simonis, R. Ulrich, S. Wayand, M. Weber, T. Weiler, S. Williamson, C. Wöhrmann, R. Wolf

Institute of Nuclear and Particle Physics (INPP), NCSR Demokritos, Aghia Paraskevi, Greece

G. Anagnostou, G. Daskalakis, T. Gerasis, A. Kyriakis, D. Loukas, G. Paspalaki, I. Topsis-Giotis

National and Kapodistrian University of Athens, Athens, Greece

G. Karathanasis, S. Kesisoglou, P. Kontaxakis, A. Panagiotou, N. Saoulidou, E. Tziaferi, K. Vellidis

National Technical University of Athens, Athens, Greece

K. Kousouris, I. Papakrivopoulos, G. Tsipolitis

University of Ioánnina, Ioannina, Greece

I. Evangelou, C. Foudas, P. Giannios, P. Katsoulis, P. Kokkas, S. Mallios, N. Manthos, I. Papadopoulos, E. Paradas, J. Strologas, F. A. Triantis, D. Tsitsonis

MTA-ELTE Lendület CMS Particle and Nuclear Physics Group, Eötvös Loránd University, Budapest, Hungary

M. Csanad, N. Filipovic, P. Major, M. I. Nagy, G. Pasztor, O. Surányi, G. I. Veres

Wigner Research Centre for Physics, Budapest, Hungary

G. Bencze, C. Hajdu, D. Horvath¹⁸, Á. Hunyadi, F. Sikler, T. Á. Vámi, V. Veszpremi, G. Vesztergombi[†]

Institute of Nuclear Research ATOMKI, Debrecen, Hungary

N. Beni, S. Czellar, J. Karancsi²⁰, A. Makovec, J. Molnar, Z. Szillasi

Institute of Physics, University of Debrecen, Debrecen, Hungary

M. Bartók¹⁹, P. Raics, Z. L. Trocsanyi, B. Ujvari

Indian Institute of Science (IISc), Bangalore, India

S. Choudhury, J. R. Komaragiri

National Institute of Science Education and Research, HBNI, Bhubaneswar, India

S. Bahinipati²¹, P. Mal, K. Mandal, A. Nayak²², D. K. Sahoo²¹, S. K. Swain

Panjab University, Chandigarh, India

S. Bansal, S. B. Beri, V. Bhatnagar, S. Chauhan, R. Chawla, N. Dhingra, R. Gupta, A. Kaur, A. Kaur, M. Kaur, S. Kaur, R. Kumar, P. Kumari, M. Lohan, A. Mehta, K. Sandeep, S. Sharma, J. B. Singh, G. Walia

University of Delhi, Delhi, India

A. Bhardwaj, B. C. Choudhary, R. B. Garg, M. Gola, S. Keshri, Ashok Kumar, S. Malhotra, M. Naimuddin, P. Priyanka, K. Ranjan, Aashaq Shah, R. Sharma

Saha Institute of Nuclear Physics, HBNI, Kolkata, India

R. Bhardwaj²³, M. Bharti, R. Bhattacharya, S. Bhattacharya, U. Bhawandeep²³, D. Bhowmik, S. Dey, S. Dutt²³, S. Dutta, S. Ghosh, K. Mondal, S. Nandan, A. Purohit, P. K. Rout, A. Roy, S. Roy Chowdhury, S. Sarkar, M. Sharan, B. Singh, S. Thakur²³

Indian Institute of Technology Madras, Madras, India

P. K. Behera

Bhabha Atomic Research Centre, Mumbai, India

R. Chudasama, D. Dutta, V. Jha, V. Kumar, P. K. Netrakanti, L. M. Pant, P. Shukla

Tata Institute of Fundamental Research-A, Mumbai, India

T. Aziz, M. A. Bhat, S. Dugad, B. Mahakud, G. B. Mohanty, N. Sur, B. Sutar, RavindraKumar Verma

Tata Institute of Fundamental Research-B, Mumbai, India

S. Banerjee, S. Bhattacharya, S. Chatterjee, P. Das, M. Guchait, Sa. Jain, S. Kumar, M. Maity²⁴, G. Majumder, K. Mazumdar, N. Sahoo, T. Sarkar²⁴

Indian Institute of Science Education and Research (IISER), Pune, India

S. Chauhan, S. Dube, V. Hegde, A. Kapoor, K. Kothekar, S. Pandey, A. Rane, S. Sharma

Institute for Research in Fundamental Sciences (IPM), Tehran, IranS. Chenarani²⁵, E. Eskandari Tadavani, S. M. Etesami²⁵, M. Khakzad, M. Mohammadi Najafabadi, M. Naseri, F. Rezaei Hosseinabadi, B. Safarzadeh²⁶, M. Zeinali**University College Dublin, Dublin, Ireland**

M. Felcini, M. Grunewald

INFN Sezione di Bari^a, Università di Bari^b, Politecnico di Bari^c, Bari, ItalyM. Abbrescia^{a,b}, C. Calabria^{a,b}, A. Colaleo^a, D. Creanza^{a,c}, L. Cristella^{a,b}, N. De Filippis^{a,c}, M. De Palma^{a,b}, A. Di Florio^{a,b}, F. Errico^{a,b}, L. Fiore^a, A. Gelmi^{a,b}, G. Iaselli^{a,c}, S. Lezki^{a,b}, G. Maggi^{a,c}, M. Maggi^a, G. Miniello^{a,b}, S. My^{a,b}, S. Nuzzo^{a,b}, A. Pompili^{a,b}, G. Pugliese^{a,c}, R. Radogna^a, A. Ranieri^a, G. Selvaggi^{a,b}, A. Sharma^a, L. Silvestris^{a,14}, R. Venditti^a, P. Verwilligen^a, G. Zito^a**INFN Sezione di Bologna^a, Università di Bologna^b, Bologna, Italy**G. Abbiendi^a, C. Battilana^{a,b}, D. Bonacorsi^{a,b}, L. Borgonovi^{a,b}, S. Braibant-Giacomelli^{a,b}, L. Brigliadori^{a,b}, R. Campanini^{a,b}, P. Capiluppi^{a,b}, A. Castro^{a,b}, F. R. Cavallo^a, S. S. Chhibra^{a,b}, G. Codispoti^{a,b}, M. Cuffiani^{a,b}, G. M. Dallavalle^a, F. Fabbri^a, A. Fanfani^{a,b}, P. Giacomelli^a, C. Grandi^a, L. Guiducci^{a,b}, S. Marcellini^a, G. Masetti^a, A. Montanari^a, F. L. Navarria^{a,b}, A. Perrotta^a, A. M. Rossi^{a,b}, T. Rovelli^{a,b}, G. P. Siroli^{a,b}, N. Tosi^a**INFN Sezione di Catania^a, Università di Catania^b, Catania, Italy**S. Albergo^{a,b}, A. Di Mattia^a, R. Potenza^{a,b}, A. Tricomi^{a,b}, C. Tuve^{a,b}**INFN Sezione di Firenze^a, Università di Firenze^b, Florence, Italy**G. Barbagli^a, K. Chatterjee^{a,b}, V. Ciulli^{a,b}, C. Civinini^a, R. D'Alessandro^{a,b}, E. Focardi^{a,b}, G. Latino, P. Lenzi^{a,b}, M. Meschini^a, S. Paoletti^a, L. Russo^{a,27}, G. Sguazzoni^a, D. Strom^a, L. Viliani^a**INFN Laboratori Nazionali di Frascati, Frascati, Italy**L. Benussi, S. Bianco, F. Fabbri, D. Piccolo, F. Primavera¹⁴**INFN Sezione di Genova^a, Università di Genova^b, Genova, Italy**F. Ferro^a, F. Ravera^{a,b}, E. Robutti^a, S. Tosi^{a,b}**INFN Sezione di Milano-Bicocca^a, Università di Milano-Bicocca^b, Milan, Italy**A. Benaglia^a, A. Beschi^b, L. Brianza^{a,b}, F. Brivio^{a,b}, V. Ciriolo^{a,b,14}, S. Di Guida^{a,d,14}, M. E. Dinardo^{a,b}, S. Fiorendi^{a,b}, S. Gennai^a, A. Ghezzi^{a,b}, P. Govoni^{a,b}, M. Malberti^{a,b}, S. Malvezzi^a, R. A. Manzoni^{a,b}, A. Massironi^{a,b}, D. Menasce^a, L. Moroni^a, M. Paganoni^{a,b}, D. Pedrini^a, S. Ragazzi^{a,b}, T. Tabarelli de Fatis^{a,b}**INFN Sezione di Napoli^a, Università di Napoli 'Federico II'^b, Napoli, Italy, Università della Basilicata^c, Potenza, Italy, Università G. Marconi^d, Rom, Italy**S. Buontempo^a, N. Cavallo^{a,c}, A. Di Crescenzo^{a,b}, F. Fabozzi^{a,c}, F. Fienga^{a,b}, G. Galati^{a,b}, A. O. M. Iorio^{a,b}, W. A. Khan^a, L. Lista^a, S. Meola^{a,d,14}, P. Paolucci^{a,14}, C. Sciacca^{a,b}, E. Voevodina^{a,b}**INFN Sezione di Padova^a, Università di Padova^b, Padova, Italy, Università di Trento^c, Trento, Italy**P. Azzi^a, N. Bacchetta^a, L. Benato^{a,b}, A. Boletti^{a,b}, A. Bragagnolo, R. Carlin^{a,b}, P. Checchia^a, M. Dall'Osso^{a,b}, P. De Castro Manzano^a, T. Dorigo^a, F. Gasparini^{a,b}, U. Gasparini^{a,b}, A. Gozzelino^a, S. Lacaprara^a, P. Lujan, M. Margoni^{a,b}, A. T. Meneguzzo^{a,b}, N. Pozzobon^{a,b}, P. Ronchese^{a,b}, R. Rossin^{a,b}, F. Simonetto^{a,b}, A. Tiko, E. Torassa^a, S. Ventura^a, M. Zanetti^{a,b}, P. Zotto^{a,b}, G. Zumerle^{a,b}**INFN Sezione di Pavia^a, Università di Pavia^b, Pavia, Italy**A. Braghieri^a, A. Magnani^a, P. Montagna^{a,b}, S. P. Ratti^{a,b}, V. Re^a, M. Ressegotti^{a,b}, C. Riccardi^{a,b}, P. Salvini^a, I. Vai^{a,b}, P. Vitulo^{a,b}**INFN Sezione di Perugia^a, Università di Perugia^b, Perugia, Italy**L. Alunni Solestizi^{a,b}, M. Biasini^{a,b}, G. M. Bilei^a, C. Cecchi^{a,b}, D. Ciangottini^{a,b}, L. Fanò^{a,b}, P. Lariccia^{a,b}, E. Manoni^a, G. Mantovani^{a,b}, V. Mariani^{a,b}, M. Menichelli^a, A. Rossi^{a,b}, A. Santocchia^{a,b}, D. Spiga^a

INFN Sezione di Pisa^a, Università di Pisa^b, Scuola Normale Superiore di Pisa^c, Pisa, Italy

K. Androsov^a, P. Azzurri^a, G. Bagliesi^a, L. Bianchini^a, T. Boccali^a, L. Borrello, R. Castaldi^a, M. A. Ciocci^{a,b}, R. Dell'Orso^a, G. Fedi^a, L. Giannini^{a,c}, A. Giassi^a, M. T. Grippo^a, F. Ligabue^{a,c}, E. Manca^{a,c}, G. Mandorli^{a,c}, A. Messineo^{a,b}, F. Palla^a, A. Rizzi^{a,b}, P. Spagnolo^a, R. Tenchini^a, G. Tonelli^{a,b}, A. Venturi^a, P. G. Verdini^a

INFN Sezione di Roma^a, Sapienza Università di Roma^b, Rome, Italy

L. Barone^{a,b}, F. Cavallari^a, M. Cipriani^{a,b}, N. Daci^a, D. Del Re^{a,b}, E. Di Marco^{a,b}, M. Diemoz^a, S. Gelli^{a,b}, E. Longo^{a,b}, B. Marzocchi^{a,b}, P. Meridiani^a, G. Organtini^{a,b}, F. Pandolfi^a, R. Paramatti^{a,b}, F. Preiato^{a,b}, S. Rahatlou^{a,b}, C. Rovelli^a, F. Santanastasio^{a,b}

INFN Sezione di Torino^a, Università di Torino^b, Torino, Italy, Università del Piemonte Orientale^c, Novara, Italy

N. Amapane^{a,b}, R. Arcidiacono^{a,c}, S. Argiro^{a,b}, M. Arneodo^{a,c}, N. Bartosik^a, R. Bellan^{a,b}, C. Biino^a, N. Cartiglia^a, F. Cenna^{a,b}, M. Costa^{a,b}, R. Covarelli^{a,b}, N. Demaria^a, B. Kiani^{a,b}, C. Mariotti^a, S. Maselli^a, E. Migliore^{a,b}, V. Monaco^{a,b}, E. Monteil^{a,b}, M. Monteno^a, M. M. Obertino^{a,b}, L. Pacher^{a,b}, N. Pastrone^a, M. Pelliccioni^a, G. L. Pinna Angioni^{a,b}, A. Romero^{a,b}, M. Ruspa^{a,c}, R. Sacchi^{a,b}, K. Shchelina^{a,b}, V. Sola^a, A. Solano^{a,b}, A. Staiano^a

INFN Sezione di Trieste^a, Università di Trieste^b, Trieste, Italy

S. Belforte^a, V. Candelise^{a,b}, M. Casarsa^a, F. Cossutti^a, G. Della Ricca^{a,b}, F. Vazzoler^{a,b}, A. Zanetti^a

Kyungpook National University, Daegu, South Korea

D. H. Kim, G. N. Kim, M. S. Kim, J. Lee, S. Lee, S. W. Lee, C. S. Moon, Y. D. Oh, S. Sekmen, D. C. Son, Y. C. Yang

Chonnam National University, Institute for Universe and Elementary Particles, Kwangju, South Korea

H. Kim, D. H. Moon, G. Oh

Hanyang University, Seoul, South Korea

J. Goh, T. J. Kim

Korea University, Seoul, South Korea

S. Cho, S. Choi, Y. Go, D. Gyun, S. Ha, B. Hong, Y. Jo, K. Lee, K. S. Lee, S. Lee, J. Lim, S. K. Park, Y. Roh

Sejong University, Seoul, South Korea

H. S. Kim

Seoul National University, Seoul, South Korea

J. Almond, J. Kim, J. S. Kim, H. Lee, K. Lee, K. Nam, S. B. Oh, B. C. Radburn-Smith, S. H. Seo, U. K. Yang, H. D. Yoo, G. B. Yu

University of Seoul, Seoul, South Korea

H. Kim, J. H. Kim, J. S. H. Lee, I. C. Park

Sungkyunkwan University, Suwon, South Korea

Y. Choi, C. Hwang, J. Lee, I. Yu

Vilnius University, Vilnius, Lithuania

V. Dudenas, A. Juodagalvis, J. Vaitkus

National Centre for Particle Physics, Universiti Malaya, Kuala Lumpur, Malaysia

I. Ahmed, Z. A. Ibrahim, M. A. B. Md Ali²⁸, F. Mohamad Idris²⁹, W. A. T. Wan Abdullah, M. N. Yusli, Z. Zolkapli

Centro de Investigacion y de Estudios Avanzados del IPN, Mexico City, Mexico

H. Castilla-Valdez, E. De La Cruz-Burelo, I. Heredia-De La Cruz³⁰, R. Lopez-Fernandez, J. Mejia Guisao, R. I. Rabadan-Trejo, G. Ramirez-Sanchez, R. Reyes-Almanza, A. Sanchez-Hernandez

Universidad Iberoamericana, Mexico City, Mexico

S. Carrillo Moreno, C. Oropeza Barrera, F. Vazquez Valencia

Benemerita Universidad Autonoma de Puebla, Puebla, Mexico

J. Eysermans, I. Pedraza, H. A. Salazar Ibarguen, C. Uribe Estrada

Universidad Autónoma de San Luis Potosí, San Luis Potosí, Mexico

A. Morelos Pineda

University of Auckland, Auckland, New Zealand

D. Krofcheck

University of Canterbury, Christchurch, New Zealand

S. Bheesette, P. H. Butler

National Centre for Physics, Quaid-I-Azam University, Islamabad, Pakistan

A. Ahmad, M. Ahmad, M. I. Asghar, Q. Hassan, H. R. Hoorani, A. Saddique, M. A. Shah, M. Shoaib, M. Waqas

National Centre for Nuclear Research, Swierk, Poland

H. Bialkowska, M. Bluj, B. Boimska, T. Frueboes, M. Górski, M. Kazana, K. Nawrocki, M. Szleper, P. Traczyk, P. Zalewski

Institute of Experimental Physics, Faculty of Physics, University of Warsaw, Warsaw, PolandK. Bunkowski, A. Byszuk³¹, K. Doroba, A. Kalinowski, M. Konecki, J. Krolikowski, M. Misiura, M. Olszewski, A. Pyskir, M. Walczak**Laboratório de Instrumentação e Física Experimental de Partículas, Lisboa, Portugal**

P. Bargassa, C. Beirão Da Cruz E Silva, A. Di Francesco, P. Faccioli, B. Galinhas, M. Gallinaro, J. Hollar, N. Leonardo, L. Lloret Iglesias, M. V. Nemallapudi, J. Seixas, G. Strong, O. Toldaiev, D. Vadrucio, J. Varela

Joint Institute for Nuclear Research, Dubna, RussiaA. Baginyan, I. Golutvin, V. Karjavin, I. Kashunin, V. Korenkov, G. Kozlov, A. Lanev, A. Malakhov, V. Matveev^{32,33}, P. Moisenz, V. Palichik, V. Perelygin, S. Shmatov, N. Skatchkov, V. Smirnov, V. Trofimov, B. S. Yuldashev³⁴, A. Zarubin, V. Zhiltsov**Petersburg Nuclear Physics Institute, Gatchina (St. Petersburg), Russia**V. Golovtsov, Y. Ivanov, V. Kim³⁵, E. Kuznetsova³⁶, P. Levchenko, V. Murzin, V. Oreshkin, I. Smirnov, D. Sosnov, V. Sulimov, L. Uvarov, S. Vavilov, A. Vorobyev**Institute for Nuclear Research, Moscow, Russia**

Yu. Andreev, A. Dermenev, S. Gninenko, N. Golubev, A. Karneyeu, M. Kirsanov, N. Krasnikov, A. Pashenkov, D. Tlisov, A. Toropin

Institute for Theoretical and Experimental Physics, Moscow, Russia

V. Epshteyn, V. Gavrilov, N. Lychkovskaya, V. Popov, I. Pozdnyakov, G. Safronov, A. Spiridonov, A. Stepenov, V. Stolin, M. Toms, E. Vlasov, A. Zhokin

Moscow Institute of Physics and Technology, Moscow, RussiaT. Aushev, A. Bylinkin³³**National Research Nuclear University 'Moscow Engineering Physics Institute' (MEPhI), Moscow, Russia**R Chistov³⁷, P. Parygin, D. Philippov, S. Polikarpov, E. Popova, E. Tarkovskii, E. Zhemchugov**P.N. Lebedev Physical Institute, Moscow, Russia**V. Andreev, M. Azarkin³³, I. Dremin³³, M. Kirakosyan³³, S. V. Rusakov, A. Terkulov**Skobeltsyn Institute of Nuclear Physics, Lomonosov Moscow State University, Moscow, Russia**

A. Baskakov, A. Belyaev, E. Boos, A. Ershov, A. Gribushin, L. Khein, V. Klyukhin, O. Kodolova, I. Lokhtin, O. Lukina, I. Miagkov, S. Obraztsov, S. Petrushanko, V. Savrin, A. Snigirev

Novosibirsk State University (NSU), Novosibirsk, RussiaV. Blinov³⁸, T. Dimova³⁸, L. Kardapoltsev³⁸, D. Shtol³⁸, Y. Skovpen³⁸**State Research Center of Russian Federation, Institute for High Energy Physics of NRC "Kurchatov Institute", Protvino, Russia**

I. Azhgirey, I. Bayshev, S. Bitioukov, D. Elumakhov, A. Godizov, V. Kachanov, A. Kalinin, D. Konstantinov, P. Mandrik, V. Petrov, R. Ryutin, S. Slabospitskii, A. Sobol, S. Troshin, N. Tyurin, A. Uzunian, A. Volkov

National Research Tomsk Polytechnic University, Tomsk, Russia

A. Babaev

University of Belgrade, Faculty of Physics and Vinca Institute of Nuclear Sciences, Belgrade, SerbiaP. Adzic³⁹, P. Cirkovic, D. Devetak, M. Dordevic, J. Milosevic**Centro de Investigaciones Energéticas Medioambientales y Tecnológicas (CIEMAT), Madrid, Spain**

J. Alcaraz Maestre, A. Álvarez Fernández, I. Bachiller, M. Barrio Luna, J. A. Brochero Cifuentes, M. Cerrada, N. Colino, B. De La Cruz, A. Delgado Peris, C. Fernandez Bedoya, J. P. Fernández Ramos, J. Flix, M. C. Fouz, O. Gonzalez Lopez, S. Goy Lopez, J. M. Hernandez, M. I. Josa, D. Moran, A. Pérez-Calero Yzquierdo, J. Puerta Pelayo, I. Redondo, L. Romero, M. S. Soares, A. Triossi

Universidad Autónoma de Madrid, Madrid, Spain

C. Albajar, J. F. de Trocóniz

Universidad de Oviedo, Oviedo, Spain

J. Cuevas, C. Erice, J. Fernandez Menendez, S. Folgueras, I. Gonzalez Caballero, J. R. González Fernández, E. Palencia Cortezon, V. Rodríguez Bouza, S. Sanchez Cruz, P. Vischia, J. M. Vizán García

Instituto de Física de Cantabria (IFCA), CSIC-Universidad de Cantabria, Santander, Spain

I. J. Cabrillo, A. Calderon, B. Chazin Quero, J. Duarte Campderros, M. Fernandez, P. J. Fernández Manteca, A. García Alonso, J. Garcia-Ferrero, G. Gomez, A. Lopez Virto, J. Marco, C. Martinez Rivero, P. Martinez Ruiz del Arbol, F. Matorras, J. Piedra Gomez, C. Prieels, T. Rodrigo, A. Ruiz-Jimeno, L. Scodellaro, N. Trevisani, I. Vila, R. Vilar Cortabitarte

CERN, European Organization for Nuclear Research, Geneva, SwitzerlandD. Abbaneo, B. Akgun, E. Auffray, P. Baillon, A. H. Ball, D. Barney, J. Bendavid, M. Bianco, A. Bocci, C. Botta, T. Camporesi, M. Cepeda, G. Cerminara, E. Chapon, Y. Chen, G. Cucciati, D. d'Enterria, A. Dabrowski, V. Daponte, A. David, A. De Roeck, N. Deelen, M. Dobson, T. du Pree, M. Dünser, N. Dupont, A. Elliott-Peisert, P. Everaerts, F. Fallavollita⁴⁰, D. Fasanella, G. Franzoni, J. Fulcher, W. Funk, D. Gigi, A. Gilbert, K. Gill, F. Glege, D. Gulhan, J. Hegeman, V. Innocente, A. Jafari, P. Janot, O. Karacheban¹⁷, J. Kieseler, V. Knünz, A. Kornmayer, M. Krammer¹, C. Lange, P. Lecoq, C. Lourenço, L. Malgeri, M. Mannelli, F. Meijers, J. A. Merlin, S. Mersi, E. Meschi, P. Milenovic⁴¹, F. Moortgat, M. Mulders, H. Neugebauer, J. Ngadiuba, S. Orfanelli, L. Orsini, F. Pantaleo¹⁴, L. Pape, E. Perez, M. Peruzzi, A. Petrilli, G. Petrucciani, A. Pfeiffer, M. Pierini, F. M. Pitters, D. Rabady, A. Racz, T. Reis, G. Rolandi⁴², M. Rovere, H. Sakulin, C. Schäfer, C. Schwick, M. Seidel, M. Selvaggi, A. Sharma, P. Silva, P. Sphicas⁴³, A. Stakia, J. Steggemann, M. Tosi, D. Treille, A. Tsiros, V. Veckalns⁴⁴, M. Verweij, W. D. Zeuner**Paul Scherrer Institut, Villigen, Switzerland**W. Bertl[†], L. Caminada⁴⁵, K. Deiters, W. Erdmann, R. Horisberger, Q. Ingram, H. C. Kaestli, D. Kotlinski, U. Langenegger, T. Rohe, S. A. Wiederkehr**ETH Zurich-Institute for Particle Physics and Astrophysics (IPA), Zurich, Switzerland**

M. Backhaus, L. Bäni, P. Berger, N. Chernyavskaya, G. Dissertori, M. Dittmar, M. Donegà, C. Dorfer, C. Grab, C. Heidegger, D. Hits, J. Hoss, T. Klijnsma, W. Lustermann, M. Marionneau, M. T. Meinhard, D. Meister, F. Micheli, P. Musella, F. Nessi-Tedaldi, J. Pata, F. Pauss, G. Perrin, L. Perrozzi, S. Pigazzini, M. Quittnat, M. Reichmann, D. Ruini, D. A. Sanz Becerra, M. Schönenberger, L. Shchutska, V. R. Tavolaro, K. Theofilatos, M. L. Vesterbacka Olsson, R. Wallny, D. H. Zhu

Universität Zürich, Zurich, SwitzerlandT. K. Aarrestad, C. Amsler⁴⁶, D. Brzhechko, M. F. Canelli, A. De Cosa, R. Del Burgo, S. Donato, C. Galloni, T. Hreus, B. Kilminster, I. Neutelings, D. Pinna, G. Rauco, P. Robmann, D. Salerno, K. Schweiger, C. Seitz, Y. Takahashi, A. Zucchetta**National Central University, Chung-Li, Taiwan**

Y. H. Chang, K. y. Cheng, T. H. Doan, Sh. Jain, R. Khurana, C. M. Kuo, W. Lin, A. Pozdnyakov, S. S. Yu

National Taiwan University (NTU), Taipei, Taiwan

P. Chang, Y. Chao, K. F. Chen, P. H. Chen, W.-S. Hou, Arun Kumar, Y. Y. Li, R.-S. Lu, E. Paganis, A. Psallidas, A. Steen, J. f. Tsai

Chulalongkorn University, Faculty of Science, Department of Physics, Bangkok, Thailand

B. Asavapibhop, N. Srimanobhas, N. Suwonjandee

Çukurova University, Physics Department, Science and Art Faculty, Adana, Turkey

A. Bat, F. Boran, S. Cerci⁴⁷, S. Damarseckin, Z. S. Demiroglu, C. Dozen, E. Eskut, S. Girgis, G. Gokbulut, Y. Guler, E. Gurpinar, I. Hos⁴⁸, E. E. Kangal⁴⁹, O. Kara, U. Kiminsu, M. Oglakci, G. Onengut, K. Ozdemir⁵⁰, S. Ozturk⁵¹, D. Sunar Cerci⁴⁷, B. Tali⁴⁷, U. G. Tok, H. Topakli⁵¹, S. Turkcapar, I. S. Zorbakir, C. Zorbilmez

Middle East Technical University, Physics Department, Ankara, Turkey

B. Isildak⁵², G. Karapinar⁵³, M. Yalvac, M. Zeyrek

Bogazici University, Istanbul, Turkey

I. O. Atakisi, E. Gülmez, M. Kaya⁵⁴, O. Kaya⁵⁵, S. Tekten, E. A. Yetkin⁵⁶

Istanbul Technical University, Istanbul, Turkey

M. N. Agaras, S. Atay, A. Cakir, K. Cankocak, Y. Komurcu, S. Sen⁵⁷

Institute for Scintillation Materials of National Academy of Science of Ukraine, Kharkov, Ukraine

B. Grynyov

National Scientific Center, Kharkov Institute of Physics and Technology, Kharkov, Ukraine

L. Levchuk

University of Bristol, Bristol, UK

T. Alexander, F. Ball, L. Beck, J. J. Brooke, D. Burns, E. Clement, D. Cussans, O. Davignon, H. Flacher, J. Goldstein, G. P. Heath, H. F. Heath, L. Kreczko, D. M. Newbold⁵⁸, S. Paramesvaran, B. Penning, T. Sakuma, D. Smith, V. J. Smith, J. Taylor

Rutherford Appleton Laboratory, Didcot, UK

K. W. Bell, A. Belyaev⁵⁹, C. Brew, R. M. Brown, D. Cieri, D. J. A. Cockerill, J. A. Coughlan, K. Harder, S. Harper, J. Linacre, E. Olaiya, D. Petyt, C. H. Shepherd-Themistocleous, A. Thea, I. R. Tomalin, T. Williams, W. J. Womersley

Imperial College, London, UK

G. Auzinger, R. Bainbridge, P. Bloch, J. Borg, S. Breeze, O. Buchmuller, A. Bundock, S. Casasso, D. Colling, L. Corpe, P. Dauncey, G. Davies, M. Della Negra, R. Di Maria, Y. Haddad, G. Hall, G. Iles, T. James, M. Komm, C. Laner, L. Lyons, A.-M. Magnan, S. Malik, A. Martelli, J. Nash⁶⁰, A. Nikitenko⁶, V. Palladino, M. Pesaresi, A. Richards, A. Rose, E. Scott, C. Seez, A. Shtipliyski, G. Singh, M. Stoye, T. Strebler, S. Summers, A. Tapper, K. Uchida, T. Virdee¹⁴, N. Wardle, D. Winterbottom, J. Wright, S. C. Zenz

Brunel University, Uxbridge, United Kingdom

J. E. Cole, P. R. Hobson, A. Khan, P. Kyberd, C. K. Mackay, A. Morton, I. D. Reid, L. Teodorescu, S. Zahid

Baylor University, Waco, USA

K. Call, J. Dittmann, K. Hatakeyama, H. Liu, C. Madrid, B. McMaster, N. Pastika, C. Smith

Catholic University of America, Washington DC, USA

R. Bartek, A. Dominguez

The University of Alabama, Tuscaloosa, USA

A. Buccilli, S. I. Cooper, C. Henderson, P. Rumerio, C. West

Boston University, Boston, USA

D. Arcaro, T. Bose, D. Gastler, D. Rankin, C. Richardson, J. Rohlf, L. Sulak, D. Zou

Brown University, Providence, USA

G. Benelli, X. Coubez, D. Cutts, M. Hadley, J. Hakala, U. Heintz, J. M. Hogan⁶¹, K. H. M. Kwok, E. Laird, G. Landsberg, J. Lee, Z. Mao, M. Narain, J. Pazzini, S. Piperov, S. Sagir⁶², R. Syarif, D. Yu

University of California, Davis, Davis, USA

R. Band, C. Brainerd, R. Breedon, D. Burns, M. Calderon De LaBarca Sanchez, M. Chertok, J. Conway, R. Conway, P. T. Cox, R. Erbacher, C. Flores, G. Funk, W. Ko, O. Kukral, R. Lander, C. Mclean, M. Mulhearn, D. Pellett, J. Pilot, S. Shalhout, M. Shi, D. Stolp, D. Taylor, K. Tos, M. Tripathi, Z. Wang, F. Zhang

University of California, Los Angeles, USA

M. Bachtis, C. Bravo, R. Cousins, A. Dasgupta, A. Florent, J. Hauser, M. Ignatenko, N. Mccoll, S. Regnard, D. Saltzberg, C. Schnaible, V. Valuev

University of California, Riverside, Riverside, USA

E. Bouvier, K. Burt, R. Clare, J. W. Gary, S. M. A. Ghiasi Shirazi, G. Hanson, G. Karapostoli, E. Kennedy, F. Lacroix, O. R. Long, M. Olmedo Negrete, M. I. Paneva, W. Si, L. Wang, H. Wei, S. Wimpenny, B. R. Yates

University of California, San Diego, La Jolla, USA

J. G. Branson, S. Cittolin, M. Derdzinski, R. Gerosa, D. Gilbert, B. Hashemi, A. Holzner, D. Klein, G. Kole, V. Krutelyov, J. Letts, M. Masciovecchio, D. Olivito, S. Padhi, M. Pieri, M. Sani, V. Sharma, S. Simon, M. Tadel, A. Vartak, S. Wasserbaech⁶³, J. Wood, F. Würthwein, A. Yagil, G. Zevi Della Porta

University of California, Santa Barbara-Department of Physics, Santa Barbara, USA

N. Amin, R. Bhandari, J. Bradmiller-Feld, C. Campagnari, M. Citron, A. Dishaw, V. Dutta, M. Franco Sevilla, L. Gouskos, R. Heller, J. Incandela, A. Ovcharova, H. Qu, J. Richman, D. Stuart, I. Suarez, S. Wang, J. Yoo

California Institute of Technology, Pasadena, USA

D. Anderson, A. Bornheim, J. Bunn, J. M. Lawhorn, H. B. Newman, T. Q. Nguyen, M. Spiropulu, J. R. Vlimant, R. Wilkinson, S. Xie, Z. Zhang, R. Y. Zhu

Carnegie Mellon University, Pittsburgh, USA

M. B. Andrews, T. Ferguson, T. Mudholkar, M. Paulini, M. Sun, I. Vorobiev, M. Weinberg

University of Colorado Boulder, Boulder, USA

J. P. Cumalat, W. T. Ford, F. Jensen, A. Johnson, M. Krohn, S. Leontsinis, E. MacDonald, T. Mulholland, K. Stenson, K. A. Ulmer, S. R. Wagner

Cornell University, Ithaca, USA

J. Alexander, J. Chaves, Y. Cheng, J. Chu, A. Datta, K. Mcdermott, N. Mirman, J. R. Patterson, D. Quach, A. Rinkevicius, A. Ryd, L. Skinnari, L. Soffi, S. M. Tan, Z. Tao, J. Thom, J. Tucker, P. Wittich, M. Zientek

Fermi National Accelerator Laboratory, Batavia, USA

S. Abdullin, M. Albrow, M. Alyari, G. Apollinari, A. Apresyan, A. Apyan, S. Banerjee, L. A. T. Bauerdick, A. Beretvas, J. Berryhill, P. C. Bhat, G. Bolla[†], K. Burkett, J. N. Butler, A. Canepa, G. B. Cerati, H. W. K. Cheung, F. Chlebana, M. Cremonesi, J. Duarte, V. D. Elvira, J. Freeman, Z. Gecse, E. Gottschalk, L. Gray, D. Green, S. Grünendahl, O. Gutsche, J. Hanlon, R. M. Harris, S. Hasegawa, J. Hirschauer, Z. Hu, B. Jayatilaka, S. Jindariani, M. Johnson, U. Joshi, B. Klima, M. J. Kortelainen, B. Kreis, S. Lammel, D. Lincoln, R. Lipton, M. Liu, T. Liu, J. Lykken, K. Maeshima, J. M. Marraffino, D. Mason, P. McBride, P. Merkel, S. Mrenna, S. Nahn, V. O'Dell, K. Pedro, C. Pena, O. Prokofyev, G. Rakness, L. Ristori, A. Savoy-Navarro⁶⁴, B. Schneider, E. Sexton-Kennedy, A. Soha, W. J. Spalding, L. Spiegel, S. Stoynev, J. Strait, N. Strobbe, L. Taylor, S. Tkaczyk, N. V. Tran, L. Uplegger, E. W. Vaandering, C. Vernieri, M. Verzocchi, R. Vidal, M. Wang, H. A. Weber, A. Whitbeck

University of Florida, Gainesville, USA

D. Acosta, P. Avery, P. Bortignon, D. Bourilkov, A. Brinkerhoff, L. Cadamuro, A. Carnes, M. Carver, D. Curry, R. D. Field, S. V. Gleyzer, B. M. Joshi, J. Konigsberg, A. Korytov, P. Ma, K. Matchev, H. Mei, G. Mitselmakher, K. Shi, D. Sperka, J. Wang, S. Wang

Florida International University, Miami, USA

Y. R. Joshi, S. Linn

Florida State University, Tallahassee, USA

A. Ackert, T. Adams, A. Askew, S. Hagopian, V. Hagopian, K. F. Johnson, T. Kolberg, G. Martinez, T. Perry, H. Prosper, A. Saha, A. Santra, V. Sharma, R. Yohay

Florida Institute of Technology, Melbourne, USA

M. M. Baarmand, V. Bhopatkar, S. Colafranceschi, M. Hohlmann, D. Noonan, M. Rahmani, T. Roy, F. Yumiceva

University of Illinois at Chicago (UIC), Chicago, USA

M. R. Adams, L. Apanasevich, D. Berry, R. R. Betts, R. Cavanaugh, X. Chen, S. Dittmer, O. Evdokimov, C. E. Gerber, D. A. Hangal, D. J. Hofman, K. Jung, J. Kamin, C. Mills, I. D. Sandoval Gonzalez, M. B. Tonjes, N. Varelas, H. Wang, Z. Wu, J. Zhang

The University of Iowa, Iowa City, USA

M. Alhusseini, B. Bilki⁶⁵, W. Clarida, K. Dilsiz⁶⁶, S. Durgut, R. P. Gandrajula, M. Haytmyradov, V. Khristenko, J.-P. Merlo, A. Mestvirishvili, A. Moeller, J. Nachtman, H. Ogul⁶⁷, Y. Onel, F. Ozok⁶⁸, A. Penzo, C. Snyder, E. Tiras, J. Wetzel

Johns Hopkins University, Baltimore, USA

B. Blumenfeld, A. Cocoros, N. Eminizer, D. Fehling, L. Feng, A. V. Gritsan, W. T. Hung, P. Maksimovic, J. Roskes, U. Sarica, M. Swartz, M. Xiao, C. You

The University of Kansas, Lawrence, USA

A. Al-bataineh, P. Baringer, A. Bean, S. Boren, J. Bowen, J. Castle, S. Khalil, A. Kropivnitskaya, D. Majumder, W. Mcbrayer, M. Murray, C. Rogan, S. Sanders, E. Schmitz, J. D. Tapia Takaki, Q. Wang

Kansas State University, Manhattan, USA

A. Ivanov, K. Kaadze, D. Kim, Y. Maravin, D. R. Mendis, T. Mitchell, A. Modak, A. Mohammadi, L. K. Saini, N. Skhirtladze

Lawrence Livermore National Laboratory, Livermore, USA

F. Rebassoo, D. Wright

University of Maryland, College Park, USA

A. Baden, O. Baron, A. Belloni, S. C. Eno, Y. Feng, C. Ferraioli, N. J. Hadley, S. Jabeen, G. Y. Jeng, R. G. Kellogg, J. Kunkle, A. C. Mignerey, F. Ricci-Tam, Y. H. Shin, A. Skuja, S. C. Tonwar, K. Wong

Massachusetts Institute of Technology, Cambridge, USA

D. Abercrombie, B. Allen, V. Azzolini, R. Barbieri, A. Baty, G. Bauer, R. Bi, S. Brandt, W. Busza, I. A. Cali, M. D'Alfonso, Z. Demiragli, G. Gomez Ceballos, M. Goncharov, P. Harris, D. Hsu, M. Hu, Y. Iiyama, G. M. Innocenti, M. Klute, D. Kovalskyi, Y.-J. Lee, A. Levin, P. D. Luckey, B. Maier, A. C. Marini, C. Mcginn, C. Mironov, S. Narayanan, X. Niu, C. Paus, C. Roland, G. Roland, G. S. F. Stephans, K. Sumorok, K. Tatar, D. Velicanu, J. Wang, T. W. Wang, B. Wyslouch, S. Zhaozhong

University of Minnesota, Minneapolis, USA

A. C. Benvenuti, R. M. Chatterjee, A. Evans, P. Hansen, S. Kalafut, Y. Kubota, Z. Lesko, J. Mans, S. Nourbakhsh, N. Ruckstuhl, R. Rusack, J. Turkewitz, M. A. Wadud

University of Mississippi, Oxford, USA

J. G. Acosta, S. Oliveros

University of Nebraska-Lincoln, Lincoln, USA

E. Avdeeva, K. Bloom, D. R. Claes, C. Fangmeier, F. Golf, R. Gonzalez Suarez, R. Kamalieddin, I. Kravchenko, J. Monroy, J. E. Siado, G. R. Snow, B. Stieger

State University of New York at Buffalo, Buffalo, USA

A. Godshalk, C. Harrington, I. Iashvili, A. Kharchilava, D. Nguyen, A. Parker, S. Rappoccio, B. Roozbahani

Northeastern University, Boston, USA

G. Alverson, E. Barberis, C. Freer, A. Hortiangtham, D. M. Morse, T. Orimoto, R. Teixeira De Lima, T. Wamorkar, B. Wang, A. Wisecarver, D. Wood

Northwestern University, Evanston, USA

S. Bhattacharya, O. Charaf, K. A. Hahn, N. Mucia, N. Odell, M. H. Schmitt, K. Sung, M. Trovato, M. Velasco

University of Notre Dame, Notre Dame, USA

R. Bucci, N. Dev, M. Hildreth, K. Hurtado Anampa, C. Jessop, D. J. Karmgard, N. Kellams, K. Lannon, W. Li, N. Loukas, N. Marinelli, F. Meng, C. Mueller, Y. Musienko³², M. Planer, A. Reinsvold, R. Ruchti, P. Siddireddy, G. Smith, S. Taroni, M. Wayne, A. Wightman, M. Wolf, A. Woodard

The Ohio State University, Columbus, USA

J. Alimena, L. Antonelli, B. Bylsma, L. S. Durkin, S. Flowers, B. Francis, A. Hart, C. Hill, W. Ji, T. Y. Ling, W. Luo, B. L. Winer, H. W. Wulsin

Princeton University, Princeton, USA

S. Cooperstein, P. Elmer, J. Hardenbrook, P. Hebda, S. Higginbotham, A. Kalogeropoulos, D. Lange, M. T. Lucchini, J. Luo, D. Marlow, K. Mei, I. Ojalvo, J. Olsen, C. Palmer, P. Piroué, J. Salfeld-Nebgen, D. Stickland, C. Tully

University of Puerto Rico, Mayagüez, USA

S. Malik, S. Norberg

Purdue University, West Lafayette, USA

A. Barker, V. E. Barnes, S. Das, L. Gutay, M. Jones, A. W. Jung, A. Khatiwada, D. H. Miller, N. Neumeister, C. C. Peng, H. Qiu, J. F. Schulte, J. Sun, F. Wang, R. Xiao, W. Xie

Purdue University Northwest, Hammond, USA

T. Cheng, J. Dolen, N. Parashar

Rice University, Houston, USA

Z. Chen, K. M. Ecklund, S. Freed, F. J. M. Geurts, M. Guilbaud, M. Kilpatrick, W. Li, B. Michlin, B. P. Padley, J. Roberts, J. Rorie, W. Shi, Z. Tu, J. Zabel, A. Zhang

University of Rochester, Rochester, USA

A. Bodek, P. de Barbaro, R. Demina, Y. t. Duh, J. L. Dulemba, C. Fallon, T. Ferbel, M. Galanti, A. Garcia-Bellido, J. Han, O. Hindrichs, A. Khukhunaishvili, K. H. Lo, P. Tan, R. Taus, M. Verzetti

Rutgers, The State University of New Jersey, Piscataway, USA

A. Agapitos, J. P. Chou, Y. Gershtein, T. A. Gómez Espinosa, E. Halkiadakis, M. Heindl, E. Hughes, S. Kaplan, R. Kunnawalkam Elayavalli, S. Kyriacou, A. Lath, R. Montalvo, K. Nash, M. Osherson, H. Saka, S. Salur, S. Schnetzer, D. Sheffield, S. Somalwar, R. Stone, S. Thomas, P. Thomassen, M. Walker

University of Tennessee, Knoxville, USA

A. G. Delannoy, J. Heideman, G. Riley, K. Rose, S. Spanier, K. Thapa

Texas A & M University, College Station, USA

O. Bouhali⁶⁹, A. Castaneda Hernandez⁶⁹, A. Celik, M. Dalchenko, M. De Mattia, A. Delgado, S. Dildick, R. Eusebi, J. Gilmore, T. Huang, T. Kamon⁷⁰, S. Luo, R. Mueller, Y. Pakhotin, R. Patel, A. Perloff, L. Perniè, D. Rathjens, A. Safonov, A. Tatarinov

Texas Tech University, Lubbock, USA

N. Akchurin, J. Damgov, F. De Guio, P. R. Duderu, S. Kunori, K. Lamichhane, S. W. Lee, T. Mengke, S. Muthumuni, T. Peltola, S. Undleeb, I. Volobouev, Z. Wang

Vanderbilt University, Nashville, USA

S. Greene, A. Gurrola, R. Janjam, W. Johns, C. Maguire, A. Melo, H. Ni, K. Padeken, J. D. Ruiz Alvarez, P. Sheldon, S. Tuo, J. Velkovska, Q. Xu

University of Virginia, Charlottesville, USA

M. W. Arenton, P. Barria, B. Cox, R. Hirosky, M. Joyce, A. Ledovskoy, H. Li, C. Neu, T. Sinthuprasith, Y. Wang, E. Wolfe, F. Xia

Wayne State University, Detroit, USA

R. Harr, P. E. Karchin, N. Poudyal, J. Sturdy, P. Thapa, S. Zaleski

University of Wisconsin-Madison, Madison, WI, USA

M. Brodski, J. Buchanan, C. Caillol, D. Carlsmith, S. Dasu, L. Dodd, S. Duric, B. Gomber, M. Grothe, M. Herndon, A. Hervé, U. Hussain, P. Klabbers, A. Lanaro, A. Levine, K. Long, R. Loveless, T. Ruggles, A. Savin, N. Smith, W. H. Smith, N. Woods

† Deceased

- 1: Also at Vienna University of Technology, Vienna, Austria
- 2: Also at IRFU, CEA, Université Paris-Saclay, Gif-sur-Yvette, France
- 3: Also at Universidade Estadual de Campinas, Campinas, Brazil
- 4: Also at Federal University of Rio Grande do Sul, Porto Alegre, Brazil
- 5: Also at Université Libre de Bruxelles, Brussel, Belgium
- 6: Also at Institute for Theoretical and Experimental Physics, Moscow, Russia
- 7: Also at Joint Institute for Nuclear Research, Dubna, Russia
- 8: Also at Fayoum University, El-Fayoum, Egypt
- 9: Now at British University in Egypt, Cairo, Egypt
- 10: Now at Ain Shams University, Cairo, Egypt
- 11: Also at Department of Physics, King Abdulaziz University, Jeddah, Saudi Arabia
- 12: Also at Université de Haute Alsace, Mulhouse, France
- 13: Also at Skobeltsyn Institute of Nuclear Physics, Lomonosov Moscow State University, Moscow, Russia
- 14: Also at CERN, European Organization for Nuclear Research, Geneva, Switzerland
- 15: Also at RWTH Aachen University, III. Physikalisches Institut A, Aachen, Germany
- 16: Also at University of Hamburg, Hamburg, Germany
- 17: Also at Brandenburg University of Technology, Cottbus, Germany
- 18: Also at Institute of Nuclear Research ATOMKI, Debrecen, Hungary
- 19: Also at MTA-ELTE Lendület CMS Particle and Nuclear Physics Group, Eötvös Loránd University, Budapest, Hungary
- 20: Also at Institute of Physics, University of Debrecen, Debrecen, Hungary
- 21: Also at Indian Institute of Technology Bhubaneswar, Bhubaneswar, India
- 22: Also at Institute of Physics, Bhubaneswar, India
- 23: Also at Shoolini University, Solan, India
- 24: Also at University of Visva-Bharati, Santiniketan, India
- 25: Also at Isfahan University of Technology, Isfahan, Iran
- 26: Also at Plasma Physics Research Center, Science and Research Branch, Islamic Azad University, Tehran, Iran
- 27: Also at Università degli Studi di Siena, Siena, Italy
- 28: Also at International Islamic University of Malaysia, Kuala Lumpur, Malaysia
- 29: Also at Malaysian Nuclear Agency; MOSTI, Kajang, Malaysia
- 30: Also at Consejo Nacional de Ciencia y Tecnología, Mexico City, Mexico
- 31: Also at Warsaw University of Technology, Institute of Electronic Systems, Warsaw, Poland
- 32: Also at Institute for Nuclear Research, Moscow, Russia
- 33: Now at National Research Nuclear University 'Moscow Engineering Physics Institute' (MEPhI), Moscow, Russia
- 34: Also at Institute of Nuclear Physics of the Uzbekistan Academy of Sciences, Tashkent, Uzbekistan
- 35: Also at St. Petersburg State Polytechnical University, St. Petersburg, Russia
- 36: Also at University of Florida, Gainesville, USA
- 37: Also at P.N. Lebedev Physical Institute, Moscow, Russia
- 38: Also at Budker Institute of Nuclear Physics, Novosibirsk, Russia
- 39: Also at Faculty of Physics, University of Belgrade, Belgrade, Serbia
- 40: Also at INFN Sezione di Pavia^a, Università di Pavia^b, Pavia, Italy
- 41: Also at University of Belgrade, Faculty of Physics and Vinca Institute of Nuclear Sciences, Belgrade, Serbia
- 42: Also at Scuola Normale e Sezione dell'INFN, Pisa, Italy
- 43: Also at National and Kapodistrian University of Athens, Athens, Greece
- 44: Also at Riga Technical University, Riga, Latvia
- 45: Also at Universität Zürich, Zurich, Switzerland
- 46: Also at Stefan Meyer Institute for Subatomic Physics (SMI), Vienna, Austria
- 47: Also at Adiyaman University, Adiyaman, Turkey

- 48: Also at Istanbul Aydin University, Istanbul, Turkey
49: Also at Mersin University, Mersin, Turkey
50: Also at Piri Reis University, Istanbul, Turkey
51: Also at Gaziosmanpasa University, Tokat, Turkey
52: Also at Ozyegin University, Istanbul, Turkey
53: Also at Izmir Institute of Technology, Izmir, Turkey
54: Also at Marmara University, Istanbul, Turkey
55: Also at Kafkas University, Kars, Turkey
56: Also at Istanbul Bilgi University, Istanbul, Turkey
57: Also at Hacettepe University, Ankara, Turkey
58: Also at Rutherford Appleton Laboratory, Didcot, UK
59: Also at School of Physics and Astronomy, University of Southampton, Southampton, UK
60: Also at Monash University, Faculty of Science, Clayton, Australia
61: Also at Bethel University, St. Paul, USA
62: Also at Karamanoğlu Mehmetbey University, Karaman, Turkey
63: Also at Utah Valley University, Orem, USA
64: Also at Purdue University, West Lafayette, USA
65: Also at Beykent University, Istanbul, Turkey
66: Also at Bingol University, Bingol, Turkey
67: Also at Sinop University, Sinop, Turkey
68: Also at Mimar Sinan University, Istanbul, Istanbul, Turkey
69: Also at Texas A&M University at Qatar, Doha, Qatar
70: Also at Kyungpook National University, Daegu, Korea